# Profit Optimization of Battery Energy Storage Systems

Emanuel Ehrlin

2024

## Acknowledgement

I want to direct gratitude towards those who have provided guidance, namely Professor Math Bollen and supervisor Fred Birath. Not to mention Erik Forsén for his guidance in the frequency regulation market.

I am truly fortunate to have had the opportunity to contribute and delve into the intricacies of this field, and for this, I extend my heartfelt thanks to Stockholm Exergi.

# Abstract

As renewable intermittent energy production becomes more prevalent, stabilizing the grid presents an increasingly complex challenge. This has led to the evolution of a lucrative frequency regulation service market and a surge in Battery Energy Storage Systems (BESS) installations. Often, there is a disparity between the prices for up- and downregulation services, and capitalizing on these price differences is crucial for maximizing profits.

This thesis proposes a bidding strategy that utilizes linear programming to enable more efficient bids on frequency regulation services, alongside energy arbitrage and peak shaving. Additionally, a frequency regulation service price forecast is developed and integrated into the algorithm, providing more informed decision-making. By employing these tools, various strategies are compared and evaluated, demonstrating the potential for increased profits through adaptive bid ratio adjustments.

# Contents

# Nomenclature

## Acronyms

| | |
|---|---|
| AEM | Alert Energy State Management |
| aFRR | automatic Frequency Restoration Reserve |
| BESS | Battery Energy Storage Systems |
| BRP | Balancing Responsible Provider |
| BSP | Balancing Service Provider |
| DOD | Depth of Discharge |
| FCR | Frequency Containtment Reserve |
| MAE | Mean Absolute Error |
| MAPE | Mean Absolute Percentage Error |
| MSE | Mean Squared Error |
| NEM | Normal Energy State Management |
| PEID | Power Electronic Interfaced Device |
| SOC | State of Charge |
| SOH | State of Health |
| SvK | Svenska Kraftnät |
| TSO | Transmission System Operator |

# 1 Introduction

The Nordic countries have set an ambition to achieve carbon-neutrality before 2050 (International Energy Agency, 2013). To reach these goals, a substantial expansion of renewable energy sources, primarily wind and solar, is projected (Energimyndigheten, 2023). However, due to the intermittency of these sources, the electricity grid has encountered increased frequency variability (Svenska kraftnät, 2024b). This, coupled with the rising electricity prices has led to a shift towards utilizing BESS to stabilize the grid. The fast ramping rate of BESS enables them to effectively provide power when needed and they are anticipated to experience significant growth in the near future (TN, 2024). Maximizing the profitability of these systems is crucial for fostering widespread expansion. Hence, the focus extends beyond grid stabilization to the provision of multiple utilities, such as energy arbitrage and peak shaving. This has the potential to stimulate a continued expansion of renewable energy sources, contributing to the gradual phase-out of fossil fuels and aiding the achievement of the climate goals.

Participating in the lucrative balancing reserve market with BESS presents a promising business opportunity today. Yet, for optimum profitability, a strategic imperative emerges: the need to craft bidding strategies that consider forecasts of balancing reserve and spot prices, while also factoring in the estimation of degradation costs. Given the relatively recent emergence of the need for such services, significant developments have taken place in the European market, prompting the need for the creation of innovative solutions.

## 1.1 Stockholm Exergi

Stockholm Exergi is a provider of electricity, district heating, and cooling services to the Stockholm region. Currently, strategic investments in BESS are done within the region. Consequently, algorithms that automate the control of these systems while maximizing their value and utility are desired.

## 1.2 Objective

The aim of this thesis is to adapt optimization techniques to the emerging developments in the frequency regulation service market in Sweden among other countries. The goal is to create a bidding algorithm that besides offering frequency regulation services, also perform energy arbitrage and peak shaving. This algorithm should bid based on a frequency regulation service price forecast. To accomplish this objective, a comprehensive understanding of market economics, battery physics, optimization methodologies, and forecasting techniques is important. To craft an effective bidding strategy, anticipating future prices is crucial. This foresight can be obtained through the utilization of machine learning, leveraging large datasets.

## 1.3 Aim of Thesis

- Develop an algorithm capable of simultaneously engaging in frequency regulation, energy arbitrage, and peak shaving.
- Generate a predictive model for frequency regulation bid prices to integrate into the algorithm.
- Conduct sensitivity analyses to determine the optimal BESS sizing and evaluate the impact of prices on profitability.

## 1.4 Scope

The primary focus lies on co-optimizing the frequency regulation services FCR and aFRR (further explained in Section 2.1) with energy arbitrage, and peak shaving. Cost calculations only include energy costs and network tariffs as they constitute the major expenses. Degradation costs are not taken into account due to time constraints. It is assumed that all frequency regulation service bids are accepted. For price forecasting, only Artificial Neural Network (ANN) and univariate Long Short-Term Memory (LSTM) models are compared, as ANN is widely used for handling large datasets and LSTM is especially effective for time series forecasts.

The remainder of this paper is organized as follows: Section 2 provides background information on how the regulation market operates, its participants, and the factors influencing service prices. Section 3 delves into the theoretical foundations of energy arbitrage, peak shaving, and frequency regulation, as well as the methodologies for cost calculations. It also discusses linear programming and outlines the necessary steps for creating a time series forecast using machine learning. Section 4 details the data preprocessing steps and the design and evaluation of both the

optimization and machine learning algorithms. In Section 5, the various bidding strategies with the optimization algorithm is compared against a simple bidding approach, and sensitivity analyses are conducted. The forecast is evaluated and compared against a naive forecast that predicts the same price as the previous day. Finally, Section 6 concludes the results and discusses the best bidding strategies and price forecast methods.

# 2 Background

In this section a background is given about frequency regulation, the different services, the market and the participation rules. The current participants are presented and details about how the main actors, i.e. the hydropower plants, affect the prices. Furthermore, a short description of the electricity market is given.

## 2.1 Frequency Regulation

The Nordic countries — Sweden, Finland, Norway, and Denmark (price zone DK-2) — share a common grid within the Nordic synchronous area, each managed by their respective Transmission System Operator (TSO): Svenska kraftnät, Fingrid, Statnett, and Energinet. The interconnected grid utilizes AC power lines, facilitating the sharing of frequency.

To maintain the stability of the grid and regulate the frequency, Balancing Service Providers (BSPs) contribute their reserves. While traditional methods in Sweden have relied on hydropower for supplying necessary power, today's grid, marked by increased instability, shows a need of rapid responses from BESS (Svenska kraftnät, 2021).

When a grid frequency deviation occurs, primary frequency regulation reserves - including FCR-N (Frequency Containment Reserve - Normal), FCR-D (Frequency Containment Reserve - Disturbance), up and down, and FFR (Fast Frequency Reserve) - are activated based on the severity of the deviation. FCR-N is a symmetric reserve activated with an effect proportional to the frequency deviation as soon as the frequency deviates from 50 Hz. In the event of a frequency deviation exceeding 0.1 Hz, FCR-D is activated - up or down - depending on the deviation direction. It is also proportional up to 0.5 Hz and operates at 100% power thereafter. As for aFRR (automatic Frequency Restoration Reserve), it is activated proportionally, up to 0.1 Hz deviation, to the frequency deviation in relation to the called off volume (Svenska kraftnät, 2024c). Refer to Table 1 for details.

| Balancing reserve | Frequency deviation (Hz) | Endurance (min) |
|---|---|---|
| FCR-N | 49.9 - 50.1 | 60 |
| FCR-D Up | 49.5 - 49.9 | 20 |
| FCR-D Down | 50.1 - 50.5 | 20 |
| aFRR Up | 49.9 - 50.0 | 60 |
| aFRR Down | 50.0 - 50.1 | 60 |

Table 1: Operation details for frequency containment reserves. The reserves operate proportionally to the extent of the frequency deviation within the specified intervals. Endurance indicates the maximum duration they are required to be able to remain activated. (Svenska kraftnät, 2024d)

Two variants of FCR-D exist: static and dynamic. The static FCR-D requires a mandatory recovery period of 15 minutes after activation, whereas the dynamic counterpart can continuously stabilize the grid without such breaks. BESS are particularly well-suited for dynamic FCR-D due to their rapid response capabilities (Svenska kraftnät, 2023c).

### 2.1.1 Compensation

The compensation mechanism varies for different services. All services receive capacity compensation, i.e. payment for the available power ready to compensate grid fluctuations, however, not all are compensated based on energy usage. Refer to Table 2 for an overview of the compensation mechanisms for various balancing services.

| Balancing service | Capacity compensation | Energy compensation |
|---|---|---|
| FCR-N | X | X |
| FCR-D | X | |
| aFRR | X | X |
| FFR | X | |
| mFRR | | X |

Table 2: Summary of balancing services and their compensation types.

For services solely receiving capacity compensation, the regulation revenue $R_{cap}^{reg}$ is determined using Equation (1), where $p_t^{service}$ represents the marginal price and $B_t$ represents the accepted bid capacity (in MW) at time $t$. For services that additionally receive compensation for activated energy $R_e^{reg}$, Equation (2) is utilized, where $p_t^{reg}$ is the regulation price (in SEK/MWh) and $E_t^{net}$ is the net delivered energy (in MWh), although this is not examined in this report.

$$R_{cap}^{reg} = \sum_{t=1}^{24} p_t^{service} B_t \tag{1}$$

$$R_e^{reg} = \sum_{t=1}^{24} p_t^{service} B_t + p_t^{reg} E_t^{net} \tag{2}$$

### 2.1.2 Limited Energy Reservoirs - LER

Limited Energy Reservoirs (LER) are units that are unable to sustain full activation for the entire duration of the pre-qualified FCR capacity, typically set at two hours (Svenska kraftnät, May 23, 2023). Special requirements are imposed on LER units participating in the FCR market to ensure their capability to supply sufficient energy and power during the contracted period. For FCR-N bidding, providers must reserve 134% of the bid power capacity in both charge and discharge directions and ensure the ability to sustain a charge and discharge for 60 minutes. In the case of FCR-D Up, providers must reserve 100% capacity in the bid direction and an additional 20% in the opposite direction. Conversely, for FCR-D Down, the requirements are reversed (Svenska kraftnät, 2023b).

This reserved extra capacity is utilized to ensure sufficient energy during operation. LER units providing FCR services are required to implement Normal State Energy Management (NEM) and Alert State Energy Management (AEM), this allows them to change the reference power (target value received from the TSO) in the following scenarios. NEM shall only be activated when the frequency is both within the normal band, i.e. ±0.1 Hz deviation of the nominal frequency 50 Hz, and the State Of Charge (SOC) is outside the range [$SOC_{enable,NEM,lower}$, $SOC_{enable,NEM,upper}$]. When it is within the range [$SOC_{disable,NEM,lower}$, $SOC_{disable,NEM,upper}$] or the frequency is outside the normal band, it should be deactivated. AEM shall be activated when the frequency is outside the normal band and when the SOC is at a critical level. Refer to Table 3 for details.

| | FCR-N | FCR-D Up | FCR-D Down |
|---|---|---|---|
| SOC enable AEM, upper | 1 - $C_{FCR-N}$ $\frac{5/60}{E}$ | N.A. | 1 - $C_{FCR-D}$ $\frac{5/60}{E}$ |
| SOC disable AEM, upper | 1 - $C_{FCR-N}$ $\frac{10/60}{E}$ | N.A. | 1 - $C_{FCR-D}$ $\frac{10/60}{E}$ |
| SOC enable NEM, upper | 1 - $C_{FCR-N}$ $\frac{30/60}{E}$ | N.A. | 1 - $C_{FCR-D}$ $\frac{20/60}{E}$ |
| SOC disable NEM, upper | 1 - $C_{FCR-N}$ $\frac{57.5/60}{E}$ | N.A. | 1 - $C_{FCR-D}$ $\frac{20/60}{E}$ |
| SOC disable NEM, lower | $C_{FCR-N}$ $\frac{10/60}{E}$ | $C_{FCR-D}$ $\frac{10/60}{E}$ | N.A. |
| SOC enable NEM, lower | $C_{FCR-N}$ $\frac{5/60}{E}$ | $C_{FCR-D}$ $\frac{5/60}{E}$ | N.A. |
| SOC disable AEM, lower | $C_{FCR-N}$ $\frac{5/60}{E}$ | $C_{FCR-D}$ $\frac{5/60}{E}$ | N.A. |
| SOC enable AEM, lower | $C_{FCR-N}$ $\frac{5/60}{E}$ | $C_{FCR-D}$ $\frac{5/60}{E}$ | N.A. |

Table 3: SOC levels of when NEM and AEM shall be activated and deactivated. $C_{FCR-X}$ is the bidded capacity in MW and $E$ is the normalized energy $E_0/E_{max}$ in MWh.

These requirements enable batteries to offer FCR block bids as opposed to aFRR, where no such requirements exist so that the SOC does not return to the initial level. However, if the batteries return to the initial level after an activation, there will be no energy compensation.

## 2.2 The Electricity Market

The majority of electricity is traded on the day-ahead market, with Nord Pool Spot being the largest platform. However, the establishment of EPEX Spot in recent times has introduced another player in the market. The system price is set for the next 24 hours every day before noon, this is the equilibrium price set by supply and demand. Zonal prices typically converge during off-peak periods such as nights and weekends, reflecting reduced electricity demand and fewer grid bottlenecks (Riksbank, 2023).

There are four electricity zones in Sweden, from SE1 in the north to SE4 in the south. With most electricity produced in the north combined with bottlenecks in the transmission grid and a predominant consumption in the south, price differences occur between zones (Energimarknadsbyrån, 2020).

### 2.2.1 Electricity Prices

Since autumn 2021, electricity prices in Sweden have remained relatively high, as seen in Figure 1. This surge can be attributed primarily to the increased price of natural gas, coupled with factors such as limited transmission line capacity, nuclear reactor maintenance, and elevated prices in neighbouring countries (Energimarknadsinspektionen, 2022).

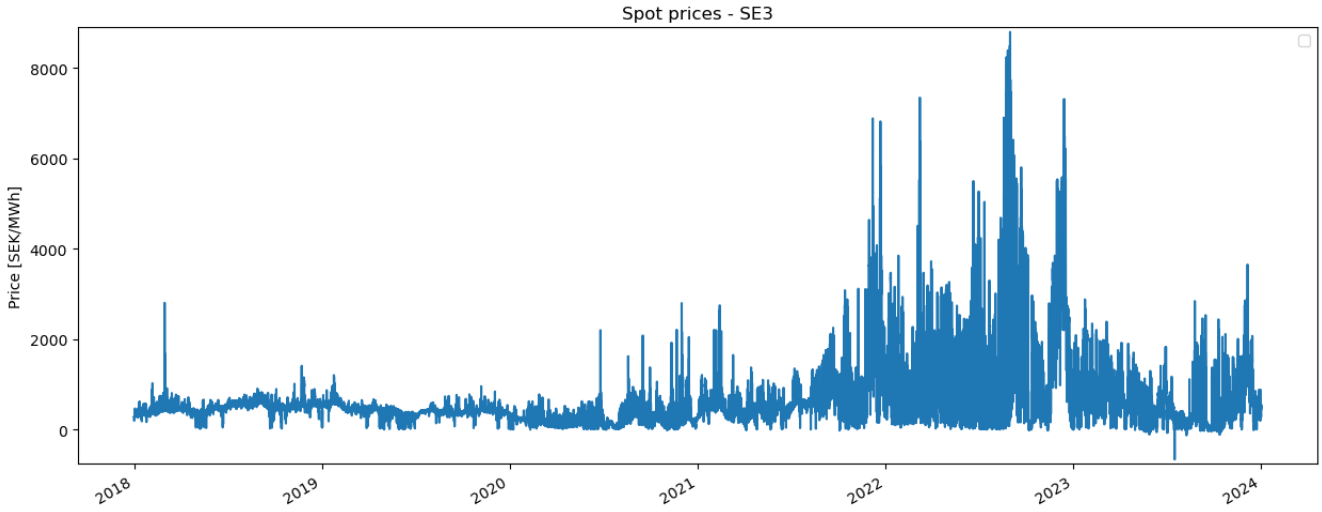


Figure 1: Hourly spot prices in SE3 from 2018 through 2023. Spot prices from (ENTSO-E, n.d.).

The projected expansion of hydrogen utilization in both the manufacturing and transportation sectors is positioned to drive an increase in electricity demand. Green hydrogen production through electrolysis, a process heavily reliant on electricity, is expected to become more economically feasible as instances of near-zero electricity prices become more frequent. Energy storage solutions like hydrogen storage, hydropower reservoirs, and batteries will play a crucial role in stabilizing electricity prices by mitigating fluctuations. With the anticipated proliferation of intermittent, weather-dependent electricity generation, despite growing energy storage capacity, electricity price volatility is expected to become more prevalent. Consequently, energy arbitrage strategies are poised to become increasingly profitable. (Riksbank, 2023).

Figures 2a to 3c illustrate the correlation between the SE2 spot price and the various services. SE2 prices are chosen due to the significant presence of regulating hydropower plants in this zone. The service prices are from Mimer (n.d.) and the spot prices from ENTSO-E (n.d.).

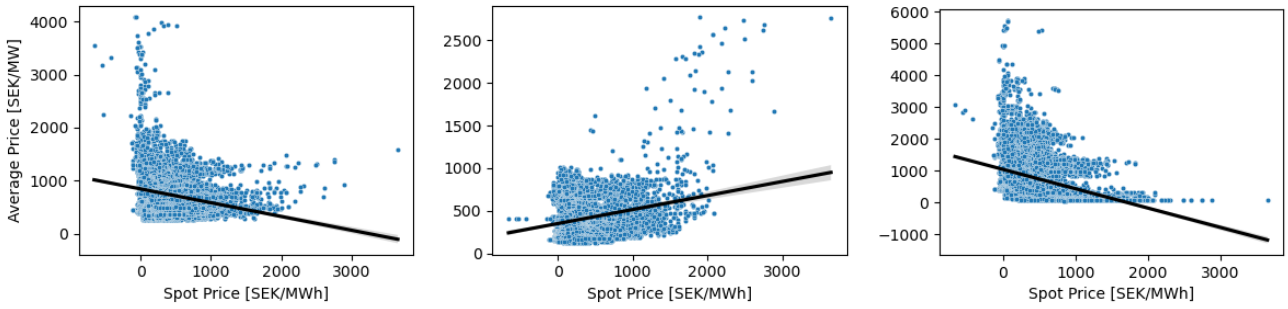


(a) FCR-N.
Correlation: -0.24.

(b) FCR-D Up.
Correlation: 0.27.

(c) FCR-D Down.
Correlation: -0.31.

Figure 2: Correlation between average FCR prices and SE2 spot prices during 2023.

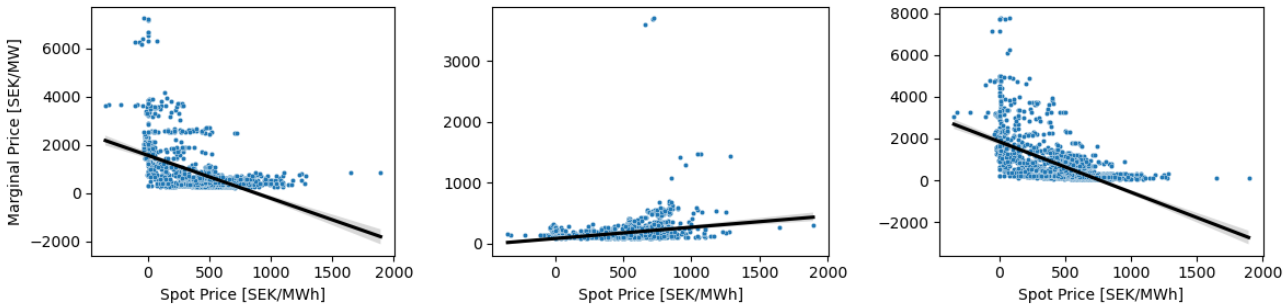


(a) FCR-N.
Correlation: -0.52.

(b) FCR-D Up.
Correlation: 0.26.

(c) FCR-D Down.
Correlation: -0.58.

Figure 3: Correlation between marginal FCR prices and SE2 spot prices from February to April 2024.

## 2.3 The Balancing Market

In the forthcoming decades, renewable energy sources such as solar and wind are anticipated to emerge as the predominant sources of power generation. While hydropower has historically served as the primary source of both power generation and flexibility, its potential to expand is limited. Consequently, BESS are expected to take on a larger share of flexibility solutions. (Svenska kraftnät, 2023f).

Solar and wind energy production is characterized not only by intermittency but also by being Power Electronic Interfaced Devices (PEID). Unlike traditional synchronous machines, PEID devices have low inertia, leading to more pronounced frequency disturbances and oscillations in response to sudden generation losses. (Svenska kraftnät, 2023f). A sample of the grid frequency is displayed in Figure 4, showing the first week of 2023.

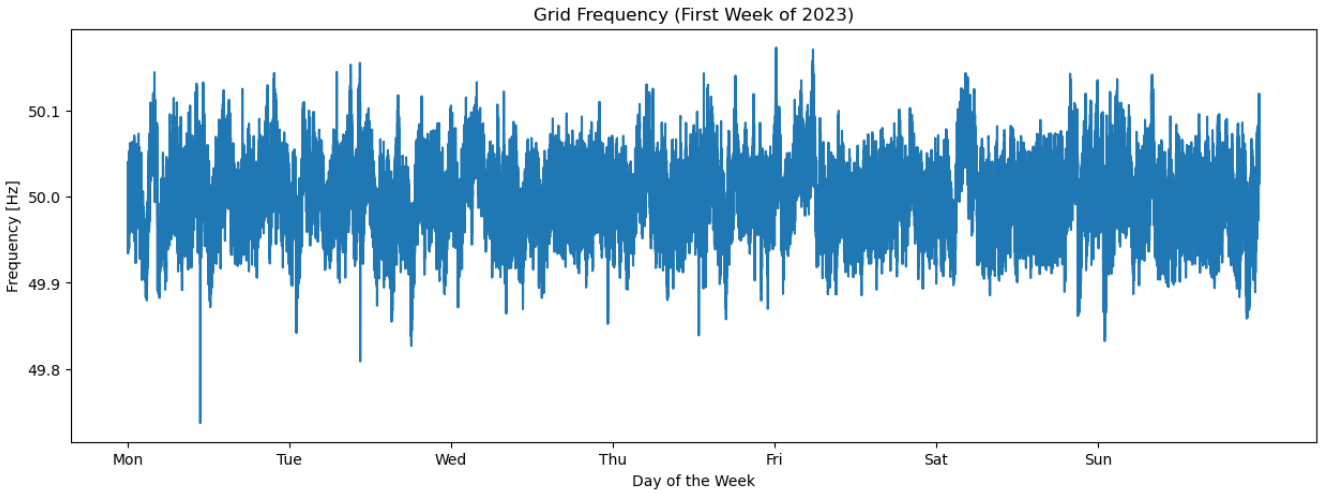


Figure 4: Nordic grid frequency from January 2nd to 8th 2023.

### 2.3.1 Hydropower Regulation

It is important to understand the factors determining the participation of hydropower in the regulation market, given that it is the main supplier of all regulation services, as illustrated in Table 4. With this knowledge, it is possible to analyse its ability to regulate given its circumstances and consequently the service prices.

| Power sources | FFR | FCR-N | FCR-D Up | FCR-D Down | aFRR Up | aFRR Down | mFRR Up | mFRR Down |
|---|---|---|---|---|---|---|---|---|
| Hydro | 0 | 1830 | 2650 | 1400 | 2680 | 2700 | 14700 | 14670 |
| Thermal | 0 | 40 | 50 | 50 | 0 | 0 | 420 | 250 |
| Energy storage | 210 | 10 | 140 | 120 | 0 | 0 | <10 | 20 |
| Flexible consumption | 100 | <10 | 520 | 10 | 0 | 0 | 200 | 120 |
| Solar | 0 | 0 | 0 | 30 | 0 | 0 | 0 | 0 |
| Wind | 0 | 150 | 210 | 500 | 0 | 250 | 340 | 850 |
| Combined hydropower & battery | 0 | 20 | 20 | 10 | 0 | 0 | 0 | 0 |
| Combined solar & energy storage | 0 | 0 | <10 | <10 | 0 | 0 | 0 | 0 |

Table 4: Pre-qualified supply (in MW) of regulation capacity by various power sources (Svenska kraftnät, 2024e).

There are more than 2000 hydropower plants in Sweden, with 80% of electricity generation from hydropower originating from Norrland. However, the expansion of Swedish hydropower has stagnated in recent decades, with most plants built during the 1950s to 1970s and the last major plant commissioned in 1994. (Swedish Energy Association, 2023).

Sweden's installed hydropower capacity has remained around 16 GW since the mid-1980s. Besides generating electricity, hydropower, thanks to its reservoirs, can regulate its generation to adapt to demand fluctuations. The diurnal power variation is typically 6-7 GW, primarily due to varying electricity consumption but increasingly influenced by intermittent electricity generation. (Swedish Energy Association, 2017).

The ability of hydropower to regulate varies among plants and throughout the year. For instance, when inflows are substantial, plants with small reservoirs prioritize electricity generation due to limited storage capacity, resulting in reduced regulation capabilities. Conversely, during periods of low inflow, such as winter, hydropower plants typically exhibit improved regulation capabilities. Additionally, this capacity is constrained by the extent of necessary production adjustments from day to day. (Swedish Energy Association, 2017).

Due to the seasonal variation in hydrological processes, the flexibility reduction observed in northern hydropower

plants during the spring flood season is counterbalanced by the enhanced flexibility seen in southern plants. Furthermore, the regulation contribution is composed of different complementary attributes, such as the speed, volume and repeatability (Swedish Energy Association, 2017). Figure 5 visually contrasts the fluctuating hydropower reservoir levels with their respective average levels.

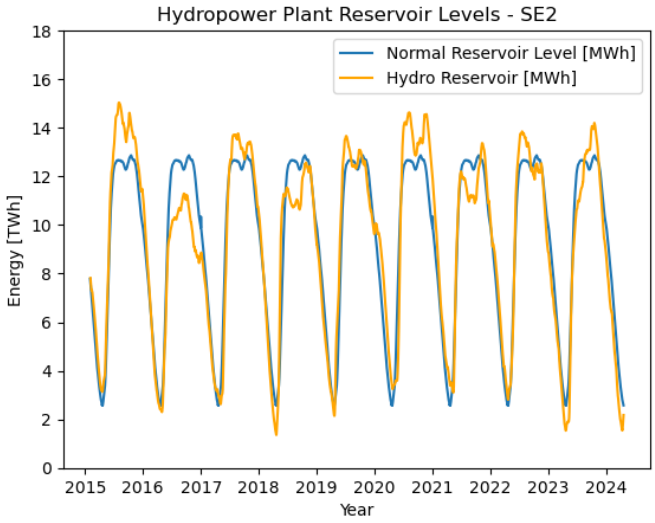


Figure 5: Aggregated hydropower reservoir levels in SE2 compared to normal average levels.

As mentioned earlier, the circumstances surrounding hydropower significantly impact service prices. The figures below illustrate the correlation between prices and different hydropower variables, used in the price forecast described in Section 4.3. In Figures 6a through 7c, scatter plots illustrate the relationship between FCR prices and aggregated hydropower reservoir levels in price zone SE2. Figures 6a to 6c display hourly average prices for the year 2023, while Figures 7a to 7c depict marginal prices from February to April 2024. Section 2.3.6 explores why there are two types of prices: average and marginal.

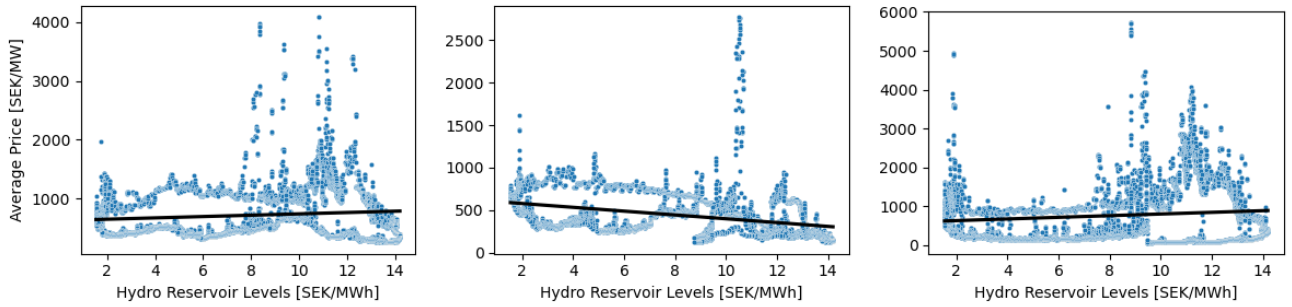


(a) FCR-N. Correlation: 0.11.

(b) FCR-D Up. Correlation: -0.39.

(c) FCR-D Down. Correlation: 0.11.

Figure 6: Correlation between average FCR prices and SE2 hydropower reservoir levels during 2023.

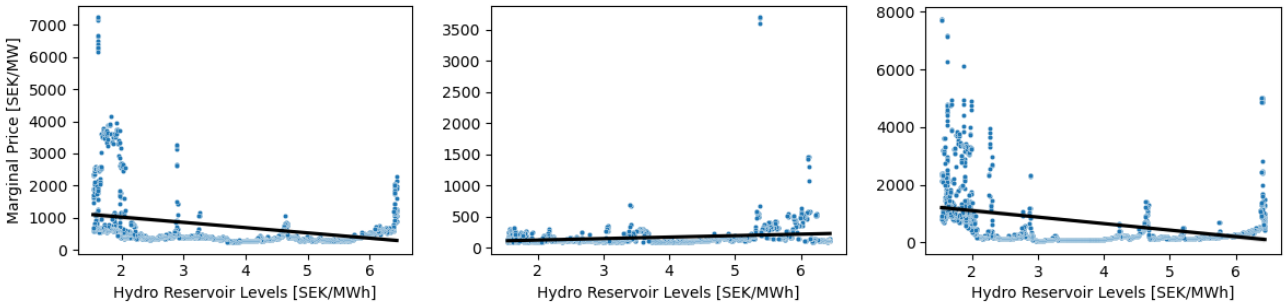


(a) FCR-N.
Correlation: -0.3.

(b) FCR-D Up.
Correlation: 0.21.

(c) FCR-D Down.
Correlation: -0.34.

Figure 7: Correlation between marginal FCR prices and SE2 hydropower reservoir levels from February to April 2024.

Figures 8a-8c suggests that a stronger correlation can be found if the hydropower reservoir levels instead are expressed as a percentage of normal levels. However, this is not the case for the marginal prices in 2024, illustrated in Figures 9a-9c. This feature engineering can be beneficial when used as input to the ANN.

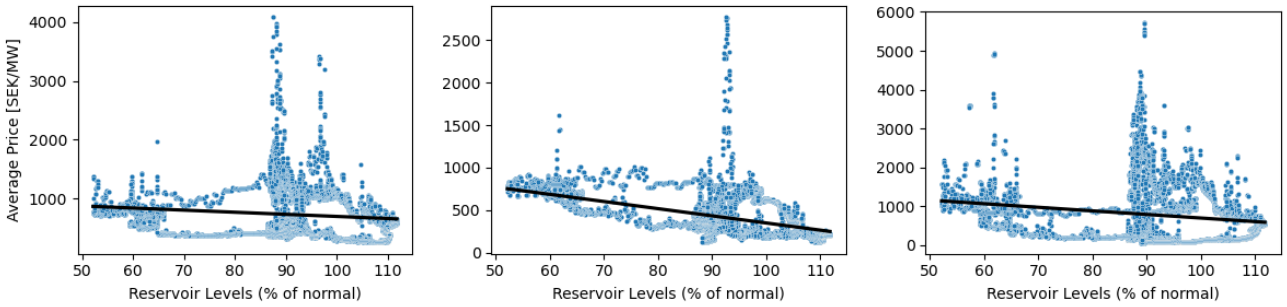


(a) FCR-N.
Correlation: -0.11.

(b) FCR-D Up.
Correlation: -0.48.

(c) FCR-D Down.
Correlation: -0.16.

Figure 8: Correlation between average FCR prices and SE2 hydropower reservoir levels as a percentage of normal levels during 2023.

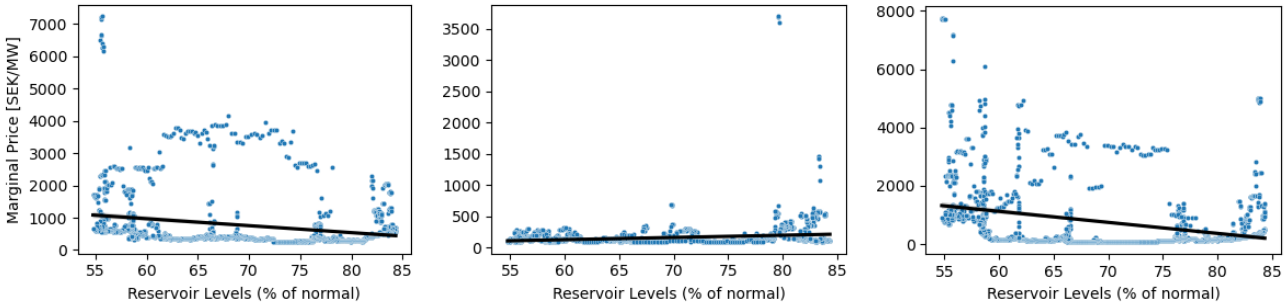


(a) FCR-N.
Correlation: -0.23.

(b) FCR-D Up.
Correlation: 0.18.

(c) FCR-D Down.
Correlation: -0.33.

Figure 9: Correlation between marginal FCR prices and SE2 hydropower reservoir levels as a percentage of normal levels during 2024.

Compared to the reservoir levels, the correlation is generally stronger between the service prices and the reservoir level change. See Figures 10a-11c.

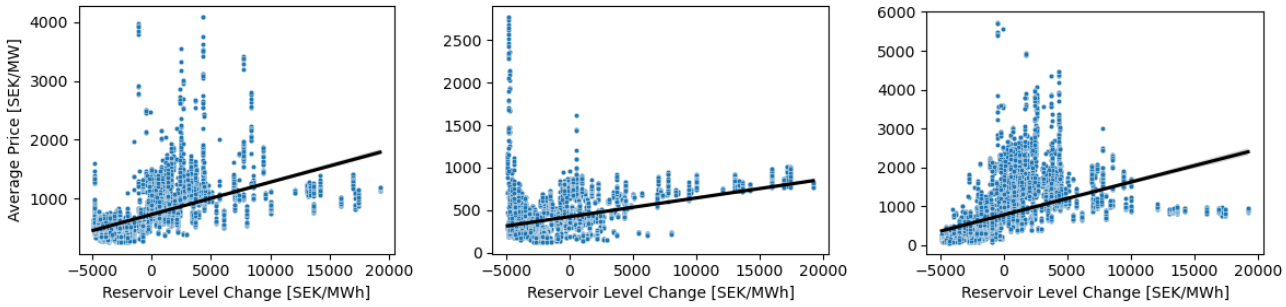


(a) FCR-N. Correlation: 0.56.

(b) FCR-D Up. Correlation: 0.41.

(c) FCR-D Down. Correlation: 0.48.

Figure 10: Correlation between average FCR prices and SE2 hydropower reservoir level changes during 2023.

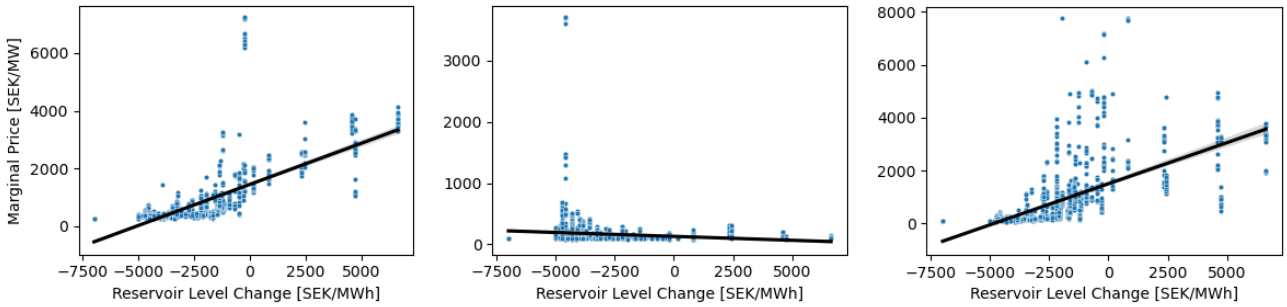


(a) FCR-N. Correlation: 0.75.

(b) FCR-D Up. Correlation: -0.16.

(c) FCR-D Down. Correlation: 0.67.

Figure 11: Correlation between marginal FCR prices and SE2 hydropower reservoir level changes from February to April 2024.

### 2.3.2 Wind Power Regulation

As noted in Table 4, wind power provides FCR services, mostly FCR-D Down. The correlation between service prices and wind power production is plotted in Figures 12a-13c.

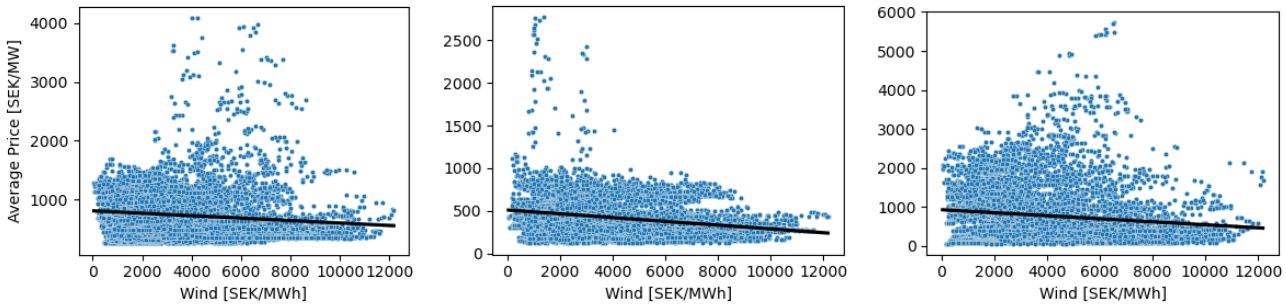


(a) FCR-N. Correlation: -0.12.

(b) FCR-D Up. Correlation: -0.24.

(c) FCR-D Down. Correlation: -0.13.

Figure 12: Correlation between average FCR prices and wind power production during 2023.

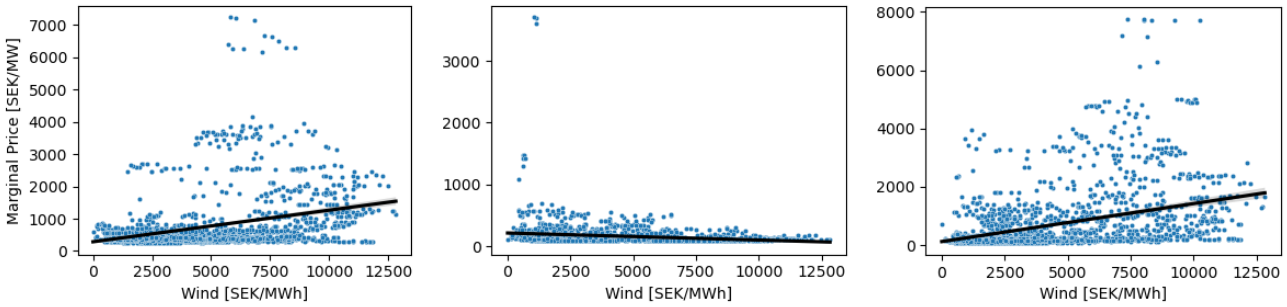


(a) FCR-N. Correlation: 0.33.

(b) FCR-D Up. Correlation: -0.18.

(c) FCR-D Down. Correlation: 0.35.

Figure 13: Correlation between marginal FCR prices and wind power production from February to April 2024.

### 2.3.3 Regulation Procurements

The procurement amounts for FCR-N and FCR-D up have been relatively stable since 2021, compared to FCR-D Down, introduced in early 2022. In contrast, the procurement amounts for aFRR have been more volatile in 2023 compared to previous years. This can be seen in Figures 14a to 14e.

The procurement of FCR-D Up is based on the largest design error in the system and can vary. For example, when Sweden's largest nuclear reactor, Oskarshamn 3, is in full operation, it generates 1450 MW. Since the grid frequency is shared among the Nordic countries, this procurement is distributed between them. Similarly, for FCR-D Down, the procurement is set at 1400 MW, matching the capacity of both North Sea Link and Nordlink (Svenska kraftnät, 2023a). The hourly procurement of FCR-D Down is expected to increase to 550 MW from today's 400 MW, and to 200 MW for aFRR Up and Down from today's 150 MW (Svenska kraftnät, 2024a).

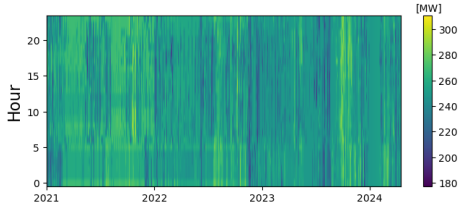


(a) Procured FCR-N.

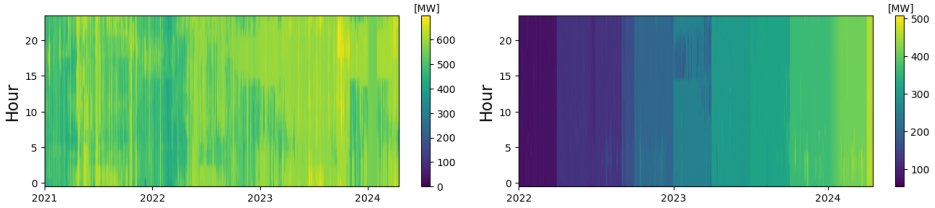


(b) Procured FCR-D Up.

(c) Procured FCR-D Down.

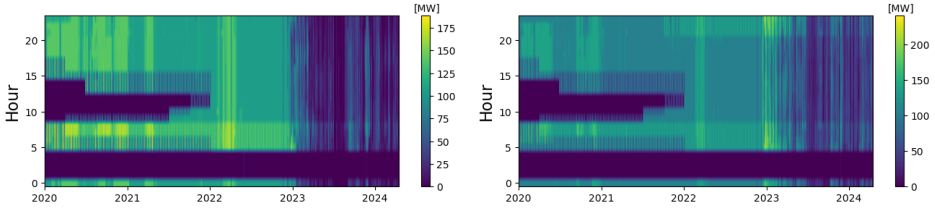


(d) Procured aFRR Up.

(e) Procured aFRR Down.

Figure 14: Swedish procurement of FCR-N, FCR-D Up, FCR-D Down, aFRR Up, and aFRR Down from 2020 through 2023. Data gathered from Mimer (n.d.).

The total Nordic procurements for aFRR is 300 MW or 400 MW depending on time of day and day of week, these procurements are split among the Nordic countries as well as the bidding zones and have remained relatively constant. The procurements are updated every quarter, for example in Q2 2023 the procurements were split as in Table 5.

| | aFRR Up | | aFRR Down | |
|---|---|---|---|---|
| Total Nordic volume | 300 | 400 | 300 | 400 |
| SE1 | 17 | 23 | 19 | 25 |
| SE2 | 16 | 22 | 19 | 25 |
| SE3 | 21 | 28 | 20 | 27 |
| SE4 | 25 | 33 | 25 | 34 |
| Total, Sweden | 79 | 106 | 83 | 111 |

Table 5: Procured volumes in MW for aFRR in Q2 2023 (Svenska kraftnät, 2023g).

### 2.3.4 Activated Energies

Activated energy is how much energy is transferred to (up activation) or from (down activation) the grid. From Figures 15a-15d it is clear that aFRR participation results in more activation than FCR. Thus, participating on the aFRR market will result in greater degradation on the BESS compared to FCR. Here, it is assumed that FCR-N is responsible for all activations since FCR-D activations are negligible in comparison. During 2022 the frequency was outside the range 49.9-50.1 Hz, where FCR-D is activated, for 9600 minutes according to Fingrid (2022). The data in Figures 15a-15d is taken from ENTSO-E (n.d.) and represent the average hourly net energy transferred to the grid for FCR and aFRR.

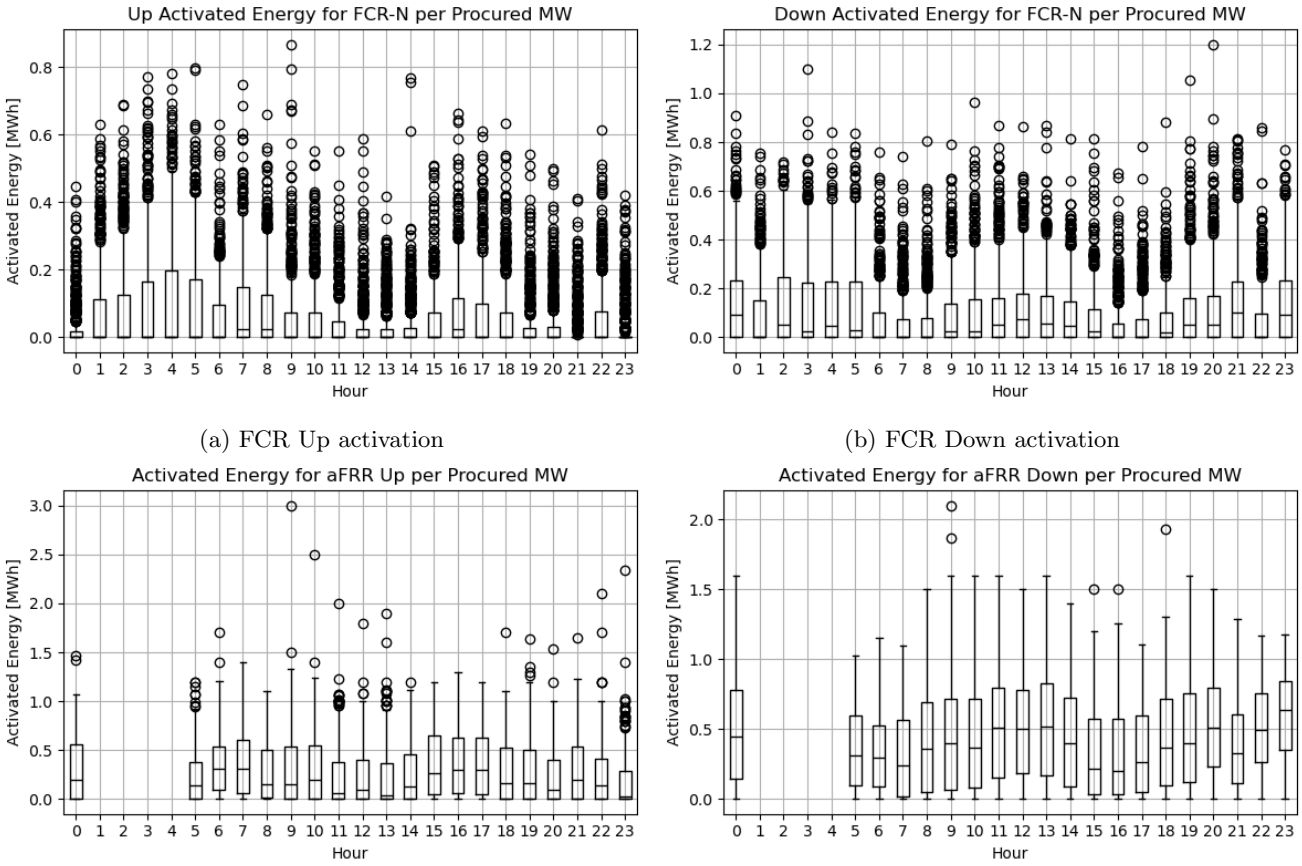


(a) FCR Up activation

(b) FCR Down activation

(c) aFRR Up activation

(d) aFRR Down activation

Figure 15: The top two plots illustrate the total FCR activated energy per procured FCR-N. Bottom plots show activated energy for aFRR Up and Down.

### 2.3.5 Regulation Service Prices

In Figure 16a-16e, hourly average price data are collected from Mimer (n.d.), and are converted to SEK, using a conversion rate of 11 SEK/€. To enhance the readability, aFRR prices above the 99.9th percentile are excluded. Additionally, due to lack of procurement, prices for aFRR services are not available for all dates.

It is worth mentioning the consistent trend of higher FCR prices observed during the summer months, a pattern that has persisted in recent years. These elevated prices can be attributed to various factors. One significant contributor is the surge in electricity prices throughout 2022. Additionally, the substantial rise in renewable energy sources like solar and wind may play a role, given their inherent lack of inertia in the electricity system and their intermittent nature. Another explanation as to why prices surge during the summer months may be due to less consumption and production, leading to fewer participants on the market.

The balancing costs that SvK faces are expected to exceed those of 2023 in 2024. According to information from TN (2024), the increased costs in 2023 were primarily attributed to heightened procurement rather than a surge in intermittent electricity generation. Currently, there is an ongoing expansion of BESS installations, which primarily aims at providing FCR services. The price trends for each service are illustrated in Figures 16a-16e. Note that these are the average prices from the former pay-as-bid market.

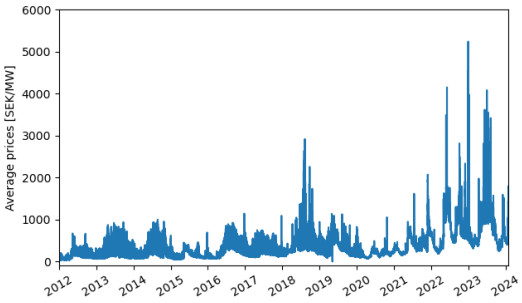


(a) FCR-N prices.

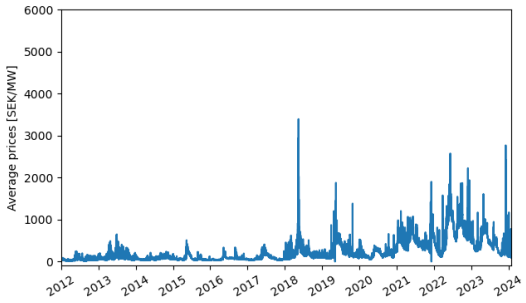


(b) FCR-D Up prices.

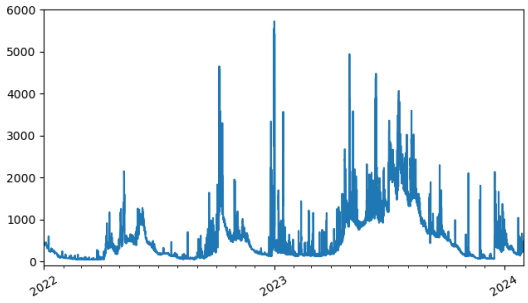


(c) FCR-D Down prices.

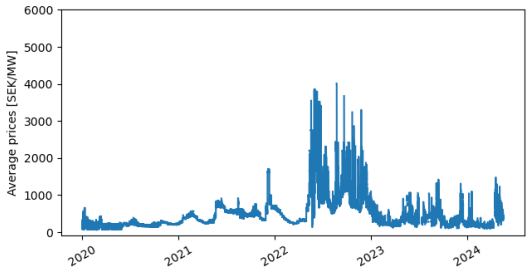


(d) aFRR Up prices.

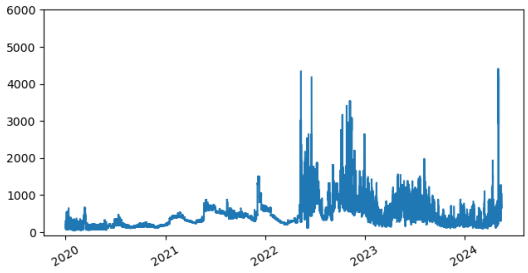


(e) aFRR Down prices.

Figure 16: Average frequency regulation service prices. Gaps in the data are due to lack of procurement and aFRR prices above the 99.9th percentile are removed due to being extreme outliers. The data is gathered from ENTSO-E (n.d.).

In Figures 17a-17c the average prices from 2020 through 2023 for the different services are visualized in heatmaps, note that prices for FCR-D Down is only available from 2022. To increase the contrast, outliers in the 99th percentile

have been removed. In Figures 18a-18c the marginal prices for FCR services are shown from February through May 2024. Recurrent patterns can be observed, for example, high FCR-N and FCR-D Down prices are more often observed in the early morning and high FCR-D Up prices later in the day.

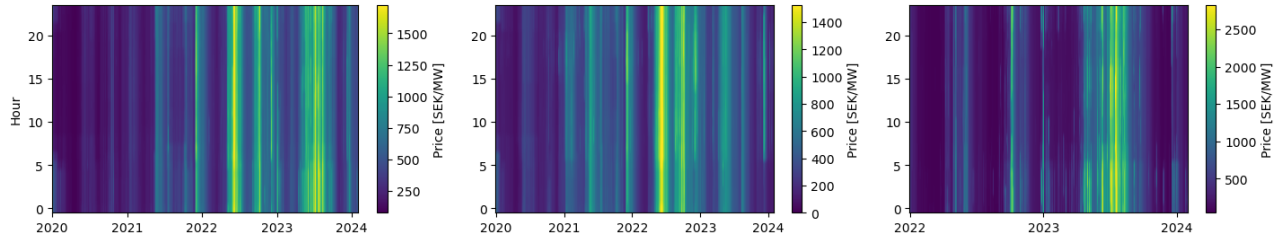


(a) FCR-N (b) FCR-D Up (c) FCR-D Down

Figure 17: Heatmaps of average prices for FCR-N and FCR-D Up from 2020 through January 2024, with FCR-D Down prices covering the period from 2022 through January 2024.

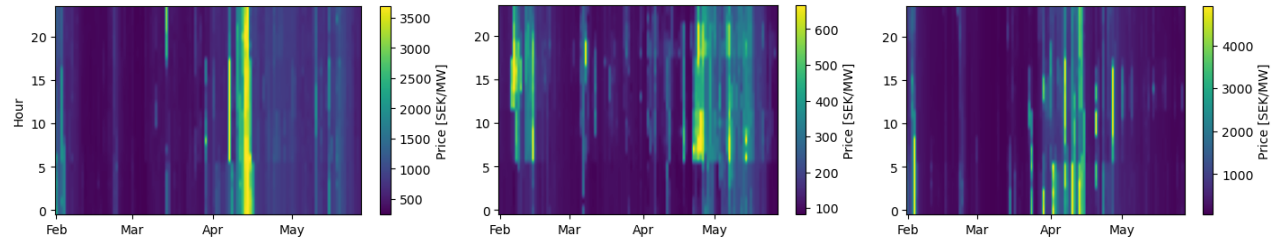


(a) FCR-N (b) FCR-D Up (c) FCR-D Down

Figure 18: Heatmaps of marginal prices for FCR-N, FCR-D Up and FCR-D Down from February through May 2024.

### 2.3.6 Market Developments

Significant changes are underway in restructuring the capacity market, and in 2024, a unified Nordic capacity market, Fifty Nordic MMS, will incorporate both aFRR and FCR services (Svenska kraftnät, 2023d). Simultaneously, FCR is transitioning from a pay-as-bid to a pay-as-clear model, where the marginal bid price determines compensation and since 2022, a new service called FCR-D Down has been introduced into the market (Svenska kraftnät, 2023e). In alignment with the rest of the European Union, the time resolution of balancing market bids, in the day-ahead markets, will in 2025 be adjusted from 60 minutes to 15 minutes (Svenska kraftnät, 2024f). In 2024, two new roles are introduced: the Balancing Responsible Party (BRP) and the Balancing Service Provider (BSP). BRPs are economically accountable for any imbalances caused by market actors, while BSPs are responsible for providing the balancing reserves FCR, aFRR and mFRR. (Svenska kraftnät, 2024f).

### 2.3.7 Market Process

There are three auctions with their own timelines, meaning that they have their own gate opening times, gate closure times and publication times. The BSPs can submit and update their bids in the bidding period between gate opening time and gate closure time and are allowed to transfer and/or repurchase their obligations to provide balancing capacity from the first to the second auction. Market clearing runs after gate closure time and the bids are selected and published to BSPs and TSOs. (Svenska kraftnät, 2022).

The bid quantity must be a multiple of the quantity factor, given by the market parameters. It must also be between the minimum and maximum quantity. There are three types of bids: single bids, block bids and bid curves. Single bids are submitted for one time period, one direction and are a multiple of the minimum quantity of 1 MW. These are indivisible, meaning that they are either accepted as a whole or rejected. Block bids on the other hand represent several single bids over multiple consecutive time periods, they have the same quantity, price and direction. These can either be indivisible or divisible. If divisible, all bids are equally divided. If block bids are undesired, the BSP

can submit a bid curve, consisting of multiple bid quantities with varying sizes for a single time period, where only one bid is accepted. (Svenska kraftnät, 2022). FCR bids are indivisible and can be submitted as block bids (ENTSO-E, 2022). aFRR bids can be either single bids, block bids or a bid curve.

## 2.4 Electricity Generation and Consumption

Electricity consumption fluctuates throughout the day, typically peaking in the morning and evening while tapering off during the mid-day. Conversely, generation often peaks during daylight hours due to solar power. This variance in net load gives rise to the infamous duck curve, which is illustrated in Figure 19. Installing BESS can flatten this curve, resulting in more stable electricity prices. Without such measures, the electricity grid may face strain during periods of overgeneration, particularly during the day. Additionally, meeting the ramp rate required to fulfill evening demand poses a challenge. (Karlsson, 2023).

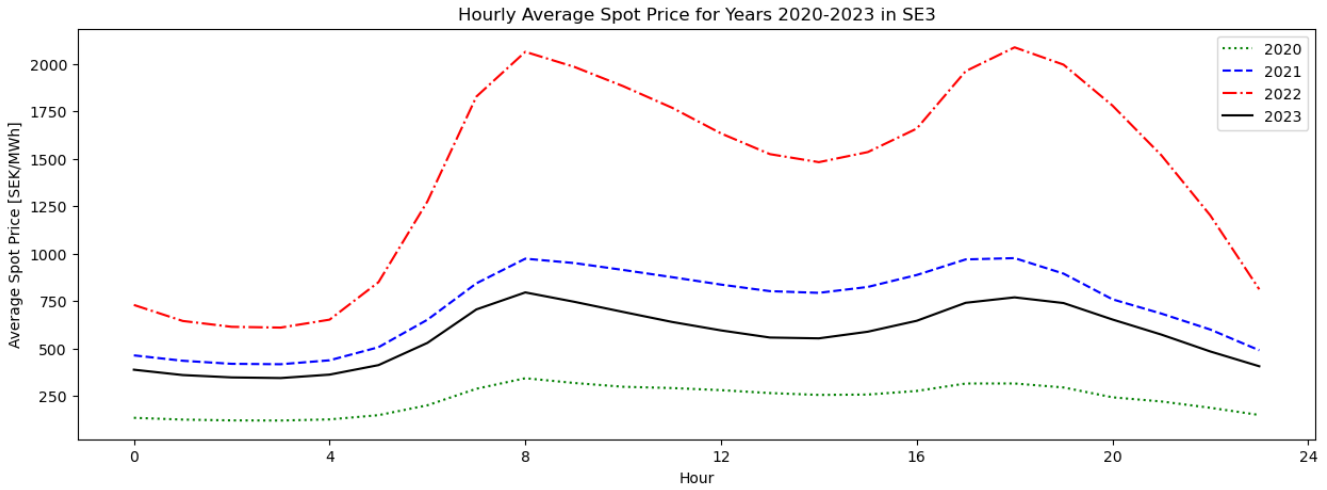


Figure 19: Hourly daily spot prices for years 2020-2023 in SE3. The shape of the curve is often referred to as the duck curve.

In addition to solar power, the remaining electricity generation is also heavily reliant on weather conditions. Hydroelectric power plants are dependent on rainfall and snowmelt, while wind power plants are depending upon wind intensity. Similarly, combined heat and power plants rely on district heat production. This weather dependence is reflected in electricity price variations, with prices typically lower during the summer and higher in the winter. (Energiföretagen Sverige, 2022).

# 3 Theory

The following is about the different services a BESS can perform besides frequency regulation, i.e. energy arbitrage and peak shaving. The section also describes the fundamentals of linear programming and forecasting methods.

## 3.1 Energy Arbitrage

Energy arbitrage is a strategy in the energy market, allowing stakeholders to capitalize on fluctuations in electricity prices by buying low and selling high. This strategy is relevant for energy storage systems, such as batteries, which can store excess energy during periods of low demand and discharge it when prices are higher.

The arbitrage revenue ($R^e$) from energy arbitrage can be calculated using Equation (3), where $p_t^e$ represents the price of electricity at time $t$, $P_t^{dis}$ denotes the power or quantity of electricity sold, and $P_t^{ch}$ indicates the amount of electricity purchased. It is important to note that the battery cannot charge and discharge simultaneously.

$$\begin{aligned} R^e &= \sum_{t=1}^{24} p_t^e (P_t^{dis} - P_t^{ch}) \\ P_t^{ch} &\cdot P_t^{dis} = 0 \end{aligned} \tag{3}$$

This equation represents the revenue generated from energy arbitrage, taking into account the difference between the selling and buying prices of electricity over a 24-hour period. The constraint $P_t^{ch} \cdot P_t^{dis} = 0$ ensures that the battery cannot charge and discharge simultaneously. For Swedish BESS, all energy taxes are refunded for inserted electricity that previously has been extracted from the grid (Skatteverket, 2024).

## 3.2 Peak Shaving

Before 2027, all Swedish electricity distribution companies are required to introduce a power tariff which brings incentives for the consumer to spread out their consumption, effectively shaving peak loads. This helps to alleviate capacity shortages in the grid by varying the fee to reflect the actual strain on the grid (Energi Informationsservice, 2022).

Energy storages connected to Ellevio's grid in Stockholm are subject to fees calculated according to Equation (4) with prices from (Ellevio (2024)). Here, $C^{grid}$ represents the total network tariff, encompassing the monthly fixed fee $C_{fix}^{grid}$, the yearly fee $C_P^{grid}$ based on the maximum instantaneous power $P_{max}^{ch}$, and $C_e^{grid}$, which depends on the total amount of energy drawn from the grid.

$$\begin{aligned} C^{grid} &= C_{fix}^{grid} + C_P^{grid} + C_e^{grid} \\ &= C_{month} k_m T + C_{year}^{pow} P_{max}^{ch} k_y T + C^{ene} \sum_{t=1}^{T} P^{ch} \end{aligned} \tag{4}$$

In this formulation, $T$ is the number of hours connected to the grid, $C_{month}$ denotes the monthly fixed cost, $C_{year}^{pow}$ represents the yearly power-based fee, and $C^{ene}$ captures the energy-related charges. The constants $k_m$ and $k_y$ are the reciprocals of the number of hours in the month and year respectively.

## 3.3 Linear Programming

Linear Programming is an optimization technique that finds the optimal decision variables $\mathbf{x}$ that either minimizes or maximizes an objective function $c^T\mathbf{x}$, where c is the cost vector. For instance, the goal could be to maximize profit or minimize cost. This is subject to the constraints $A\mathbf{x} \leq b$. Here, $A$ is the constraint matrix and $b$ is the right-hand side vector. This creates a feasible region with possible solutions in a space with dimension equal to the size of $\mathbf{x}$. A common solver algorithm is the simplex method which searches along the constraints at the edge of the feasible region and converges to an optimal solution while satisfying all constraints. (Kochenderfer & Wheeler, 2019)

## 3.4 Forecasting Methods

There are several techniques that can be utilized for multivariate time series forecasting such as linear regression, boosting algorithms such as XGBoost, artificial neural networks (ANN) and recurrent neural networks such as LSTM. Neural networks are useful when large amounts of data is available, especially when there are non-linear relationships. LSTMs can also be univariate networks, having only the historical prices as input.

### 3.4.1 Feature Engineering

Preprocessing the input can sometimes lead to better performance. Cyclical encoding is a suitable method when dealing with temporal features such as hour, weekday and month. It involves performing a cosine and sine transformation as shown in equations (5)-(6), where T represents the time period.

$$x_{cos} = cos\left(\frac{2\pi x}{T}\right) \tag{5}$$

$$x_{sin} = sin\left(\frac{2\pi x}{T}\right) \tag{6}$$

Although leading to a doubling in amount of temporal features, this removes the discontinuities in the data, effectively improving the convergence speed of the network.

### 3.4.2 Hyperparameter Tuning

Achieving high-performing models involves an iterative process of assessing various feature combinations and hyperparameters, which collectively shape the architecture of the models. One crucial aspect is the learning rate, determining the speed at which the network converges. If set too high, the model's weights risk converging to a local minimum instead of the global minimum. The regularization strength is another critical factor, regulating the impact of large weights. Applying regularization helps prevent overly complex and overfitted models, thereby enhancing their ability to generalize to unseen data. However, excessive regularization can hinder the model's capacity to learn intricate patterns. Additionally, fine-tuning the number of layers and neurons per layer involves striking a balance between capturing complex patterns and avoiding overfitting. It is a delicate trade-off that requires careful consideration to ensure optimal model performance. Including dropout disables a portion of the connections between nodes, making the model less prone to overfit on the training data. Activation functions are commonly used between layers as well as on the output layer to introduce non-linearity, enabling the network to more easily learn non-linear functions. Lastly, choosing the right optimizer is important since it for example affects convergence speed, its ability to escape local minimas and the robustness to noisy gradients.

Proper tuning involves finding the best performing combinations of hyperparameters. One efficient approach is Bayesian optimization that builds a probability model of the objective function and uses it to select the most promising hyperparameters $x$ to evaluate in the true objective function. In the following function

$$x^* = arg\min_{x \in X} f(x), \tag{7}$$

the best hyperparameters $x^*$ yields the lowest score in f(x), which is the metric to minimize in the validation set, e.g. the Mean Squared Error (MSE). Bayesian optimization uses past evaluations to decide the next choice of hyperparameters to evaluate. This leads to less time needed to find the best hyperparameters compared to grid search which is a simple and common technique.

### 3.4.3 Model Selection and Evaluation

There are multiple cross-validation methods, one of them is a rolling window. It uses a training, a validation and a test window of user defined size and moves through the dataset with fixed increments. With each increment, the model is trained, validated and finally evaluated on the test set, yielding a score such as the Mean Absolute Error (MAE) or Mean Absolute Percentage Error (MAPE). The model should be selected based on the performance on the validation set. Another method is an expanding window with fixed increments but with increasing training window size. Using this method can be beneficial in situations with few data. These cross-validation methods are also known as walk-forward time series cross-validation. They are used to verify the model's performance on unseen data, i.e. the test set.

# 4 Method

The task is split into two primary components: optimization and price forecasting, both executed with Python leveraging Github Copilot, an AI-assisted pair programming tool. Websites where the data is collected is shortly detailed in Section 4.1. For the optimization phase, discussed in Section 4.2, a linear programming methodology is adopted utilizing Pyomo, a Python-based open-source optimization package known for its model creation and solving capabilities. In the price forecasting phase, covered in Section 4.3, the neural networks ANN and a univariate LSTM are explored, with implementations carried out using scikit-learn and PyTorch, machine learning libraries.

## 4.1 Data Collection

Data from various sources are aggregated to support the analysis. SvK's Mimer platform Mimer (n.d.) serves as a primary data repository, providing information on ancillary service prices, procurements, and electricity generation. Day-ahead electricity prices and activated energy for FCR and aFRR are sourced from ENTSO-E's website ENTSO-E (n.d.). Hydropower plant reservoir data are obtained from Montel's Energy Quantified website EQ Energy (2024).

## 4.2 Optimization

Maximizing profit in the energy sector requires active participation in multiple markets concurrently. To achieve this, linear programming, as described in Section 3.3, is employed to determine the optimal allocation of bid capacity across various frequency regulation services, alongside energy arbitrage and peak shaving strategies. The objective functions and its constraints are given in equations (8a) to (8f).

$$\max\ \pi = \max(R^{reg} + R^{e} - C^{grid}) \tag{8a}$$

subject to:

$$SOC_t = SOC_{t-1} + P_t^{ch}\sqrt{\eta} - \frac{P_t^{dis}}{\eta} \quad \forall t \in T \tag{8b}$$

$$SOC_t = SOC_{t+24} \quad \forall t \in T \tag{8c}$$

$$P_t^{ch} \leq P_{max}^{ch}\sqrt{\eta} \quad \forall t \in T \tag{8d}$$

$$P_t^{dis} \leq \frac{P_{max}^{dis}}{\sqrt{\eta}} \quad \forall t \in T \tag{8e}$$

$$\sum_{t=1}^{T} P_t^{dis} \leq max_{DD} \quad \forall t \in T \tag{8f}$$

In the above optimization problem, $\pi$ denotes the profit from BESS operation, $R^{reg}$ represents revenue from participation in the frequency regulation market, $R^{e}$ signifies revenue from energy arbitrage in the spot market and $C^{grid}$ encompasses network tariffs. The latter three variables are calculated in their respective equations: (1), (3) and (4). The problem is solved for each day separately due to computational constraints. Equation (8b) dictates the effect of power $P_{ch}$ and $P_{dis}$ on the SOC, while (8c) ensures SOC consistency between the beginning and the end of the day. Power limits, with the round-trip efficiency $\eta$, are defined in (8d) and (8e), while (8f) limits cycling to $max_{DD}$ cycles, with $T = 24$ representing the number of hours in a day. The decision variables are $P^{ch}$, $P^{dis}$ and the bid capacities $B_i$ while the state variable is $\text{SOC}_t$.

### 4.2.1 FCR Constraints

When participating in the FCR market with LER units, the objective function is subject to the endurance and LER constraints described in Section 2.1.2:

$$1.34B_t^{FCR-N} + B_t^{FCR-D,up} + 0.2B_t^{FCR-D,down} \leq P_{max}^{dis} - P_t^{dis} \quad \forall t \in T \tag{9a}$$

$$1.34B_t^{FCR-N} + 0.2B_t^{FCR-D,up} + B_t^{FCR-D,down} \leq P_{max}^{ch} - P_t^{ch} \quad \forall t \in T \tag{9b}$$

$$B_t^{FCR-N} + 0.33B_t^{FCR-D,up} \leq SOC_t - SOC_{min} \quad \forall t \in T \tag{9c}$$

$$B_t^{FCR-N} + 0.33B_t^{FCR-D,down} \leq SOC_{max} - SOC_t \quad \forall t \in T \tag{9d}$$

Note that $B_t$ is the accepted bid capacity, same as in Equation (1). The first two constraints ensure that the battery has enough power available in both directions whereas the third and fourth rows guarantee that the battery possesses sufficient energy and energy margin for the specified endurance. The constants 1 and 1/3 represents 60 minutes and 20 minutes respectively.

#### 4.2.2 aFRR Constraints

When engaging in the aFRR market, there is no extra power to be reserved in any direction because LER rules are not applied. The energy and power constraints are as follows:

$$B_{aFRR,up} \leq P_{max}^{dis} - P_t^{dis} \quad \forall t \in T \tag{10a}$$
$$B_{aFRR,down} \leq P_{max}^{ch} - P_t^{ch} \quad \forall t \in T \tag{10b}$$
$$B_{aFRR,up} \leq SOC_t - SOC_{min} \quad \forall t \in T \tag{10c}$$
$$B_{aFRR,down} \leq SOC_{max} - SOC_t \quad \forall t \in T \tag{10d}$$

If the BESS participates in the FCR market simultaneously, $P_t^{dis}$ and $P_t^{ch}$ can be non-zero. Binary variables are created using equations (11a)-(11e):

$$B_{FCR-N} \leq M \cdot b_t^{FCR-N} \quad \forall t \in T \tag{11a}$$
$$B_{FCR-D,up} \leq M \cdot b_t^{FCR-D,up} \quad \forall t \in T \tag{11b}$$
$$B_{FCR-D,down} \leq M \cdot b_t^{FCR-D,down} \quad \forall t \in T \tag{11c}$$
$$B_{aFRR,up} \leq M \cdot b_t^{aFRR,up} \quad \forall t \in T \tag{11d}$$
$$B_{aFRR,down} \leq M \cdot b_t^{aFRR,down} \quad \forall t \in T \tag{11e}$$

Here, M is a big number and $b$ are binary variables. To overcome the problem of not having a recovery strategy during the period, such as NEM for FCR, one strategy is to ensure that enough energy is available at the start of the period by letting the BESS to have a recovery period every other hour. This is accomplished by equations (12a)-(12f):

$$b_{t+1}^{aFRR,down} \leq M \cdot (1 - b_t^{aFRR,up}) \quad \forall t \in T \tag{12a}$$
$$b_t^{aFRR,up} + b_{t+1}^{aFRR,up} \leq 1 \quad \forall t \in T \tag{12b}$$
$$b_t^{aFRR,down} + b_{t+1}^{aFRR,down} \leq 1 \quad \forall t \in T \tag{12c}$$
$$b_t^{aFRR} \leq b_t^{aFRR,up} \quad \forall t \in T \tag{12d}$$
$$b_t^{aFRR} \leq b_t^{aFRR,down} \quad \forall t \in T \tag{12e}$$
$$b_{t+1}^{FCR-N} + b_{t+1}^{FCR-D,up} + b_{t+1}^{FCR-D,down} \leq M \cdot (1 - b_t^{aFRR}) \quad \forall t \in T \tag{12f}$$

Equations (12a)-(12c) ensure that only either the binary variable for aFRR Up or aFRR Down is active in a consecutive time step. Equations (12d) and (12e) check if any aFRR is active and if it is, (12f) restricts any other bid to be active the next time step. Moreover, binary variables are also used to prevent the battery from having non-zero power two consecutive hour, obeying LER rules. This is implemented in equations (13a)-(13c).

$$P_t^{ch} \leq M \cdot b_t^{ch} \quad \forall t \in T \tag{13a}$$
$$P_t^{dis} \leq M \cdot b_t^{dis} \quad \forall t \in T \tag{13b}$$
$$b_t^{ch} + b_{t+1}^{ch} + b_t^{dis} + b_{t+1}^{dis} \leq 1 \quad \forall t \in T \tag{13c}$$

The first two ensures that charging or discharging activates one of the respective binary variable. The third equation only let one binary variable at time $t$ or $t+1$ to be active.

#### 4.2.3 Sensitivity Analysis

The profit's and bid sizes' sensitivity to model parameters is analysed by iteratively adjusting them, resolving the objective function and observing the change in profit and type of frequency regulation service bids. The analysed parameters are the frequency regulation service price, battery capacity and power rating. The observation of profit and bid sensitivity concerning battery capacity and power rating is intriguing as it sheds light on determining the optimal sizing of the BESS. Additionally, understanding price sensitivity is crucial as it provides insights into how profits may be impacted in an evolving market landscape.

## 4.3 Frequency Regulation Service Price Forecast

To assess the feasibility of a frequency regulation service price forecast, a data analysis is undertaken as seen in Section 2. Subsequently, various methods are compared by using cross-validation together with evaluation metrics such as the MAE and MAPE. Forecasts from both ANNs and LSTMs are evaluated.

### 4.3.1 Data Analysis and Preprocessing

The input data for the ANN models include variables for which forecasts are available, including spot prices, hydropower reservoir levels and reservoir level changes as well as the hour of the day. The significance of these data is assessed through correlation analysis. The hour of the day is cyclically encoded by using Equation (5) and (6).

To train the ANN models, a rolling window cross-validation technique is employed, as described in Section 3.4.3. The training dataset consists of a window size of 7 days while the validation and test windows each span one day, thus leading to a validation set less than 20% of the total window. Here, a compromise is done between training the model on more recent data and selecting models based on their performance on the validation data. The rationale behind using a rolling window with recent observations is to adapt to evolving market conditions, rather than relying on obsolete data. Furthermore, having the training window too large can result in overfitting. A rolling window of 30 days is used for the LSTM models during 2023 due to the abundance of data, however, during 2024, when the marginal prices were introduced, an expanding window of a minimum of 10 days of training data was utilized to be able to assess the models on a longer time period. 30 days is considered enough due to time and computational resource constraints. Also, a compromise between training speed and the complexity of the model is done by limiting the hidden size and the input sequence length for the LSTM.

To ensure balanced importance of each input variable and enhance ANN model performance, the data is standardized, i.e. scaling the data to have a mean of 0 and a standard deviation of 1. The same is done for input price sequences for the LSTM. Additionally, to prevent data leakage and ensure robustness of the results, the standardization scaler is fitted solely on the training dataset. The same scaler is then applied to the validation and test dataset during the evaluation phase.

### 4.3.2 Network Architecture and Training

Bayesian optimization is utilized to identify optimal hyperparameters by minimizing the MSE validation loss across all folds as shown in Equation (7). The MSE is chosen due to the regression nature of the problem. The hyperparameters include the learning rate, regularization strength, dropout rate, number of layers and units per layer. To address the influence of outliers, which can lead to high validation losses in some folds and are often challenging to predict, the median of the losses is used instead of the mean. This hyperparameter optimization process is repeated for each price, and feature combination for the ANN, leading to a unique network architecture tailored to each price. In addition to customizing the network architecture for price forecasting, it is equally crucial to analyse how the amount of training data (for ANN) and sequence length (for LSTM) impacts performance. The optimal amount is found by employing Bayesian optimization in these aspects as well.

Additionally, multiple optimizers are evaluated such as Adam, AdamW and SGD as well as the activation functions ReLU, linear, mish and swish. Ultimately, AdamW was chosen for both ANN and LSTM because it in most cases resulted in the best performance. Additionally, for the ANN, ReLU was used between each layer and on the output while a linear activation function was used on the LSTM output. Furthermore, the initial weights are randomly set by the default Pytorch initialization method, ensuring a uniform weight distribution between $-\sqrt{k}$ and $\sqrt{k}$, where $k$ is the reciprocal of the number of input features. The random initialization contributes to the generation of indeterministic models.

The univariate sequence-to-sequence LSTM predicts 24 hours ahead, simulating real world operation, resulting in one cross-validation fold for each day. The training is stopped if the training reaches either 1000 epochs or if the validation loss does not decrease by more than 0.01% of the initial loss for 10 epochs, i.e. a patience of 10. Lastly, a batch size of 128 is used.

### 4.3.3 Evaluation

The evaluation of the models' performances on the test set involved using two key metrics: MAE and MAPE. These metrics offer an intuitive understanding of the models' accuracy compared to using the Root Mean Squared Error (RMSE), which can be more challenging to interpret. The metrics are calculated for each cross-validation

split and then averaged to provide an overall assessment of model performance. This is done 10 times, followed by another averaging to provide a more robust performance assessment. This is done due to the indeterministic nature of neural networks caused by the random weight initialization. Additionally, the models' performances are benchmarked against a naive forecast, which forecasts a price equal to that of the previous day. Following this evaluation, the forecasted prices are integrated into the optimization algorithm to assess their overall effectiveness.

# 5 Results

In this section, the price forecasting results are examined and then used in the optimization algorithm to determine its performance in various bidding strategy simulations.

## 5.1 Frequency Regulation Service Price Forecasts

The investigated forecasting methods ANN and univariate LSTM are compared against the naive model. The average price forecasts are only evaluated for the year of 2023. The marginal price forecasts are all evaluated from the 11th of February 2024 because of the expanding window used by the LSTM, this is to remove poor performance when trained on too little data. Farther than 14th of April is not forecasted. The input features that yielded the lowest median validation loss are used for the ANN forecasts.

### 5.1.1 Average FCR-N Price Forecasts

Average FCR-N price forecast results are illustrated in Figures 20a-20c. The features used for the ANN forecast are the hour of the day, SE2 spot prices, SE2 hydropower reservoir levels and wind power production. The naive forecast performs best with a MAE of 92 SEK/MW.

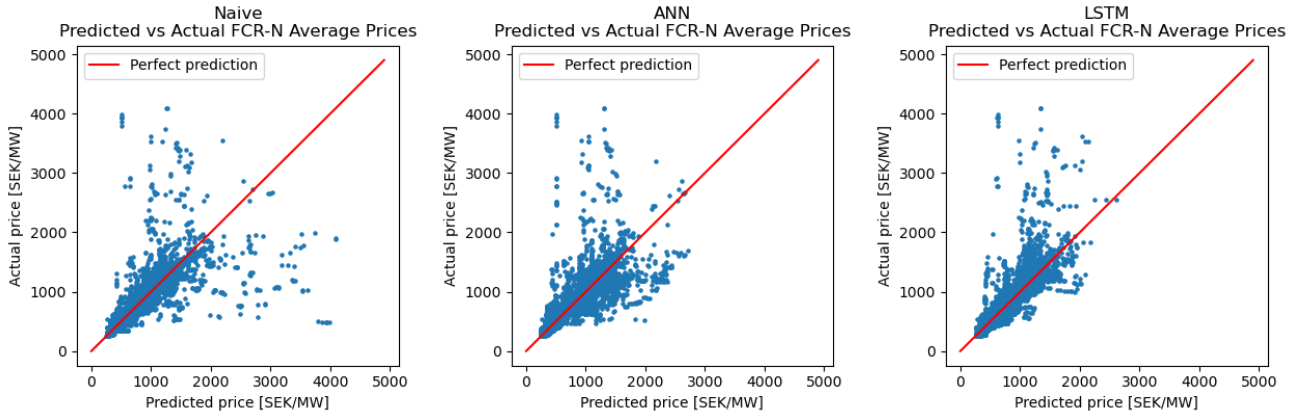


(a) Naive forecast with MAE: 92 SEK/MW and MAPE: 10 %

(b) ANN forecast with MAE: 127.5 SEK/MW and MAPE: 14.3 %

(c) LSTM forecast with MAE: 103.7 SEK/MW and MAPE: 11.2 %

Figure 20: Average FCR-N price forecasting results for the year of 2023.

### 5.1.2 Marginal FCR-N Price Forecasts

Marginal FCR-N price forecast results are illustrated in Figures 21a-21c. The features used for the ANN forecast are the SE2 spot prices, SE2 hydropower reservoir level as a percentage of normal levels and its derivative. The LSTM forecast performs best with a MAE of 255 SEK/MW.

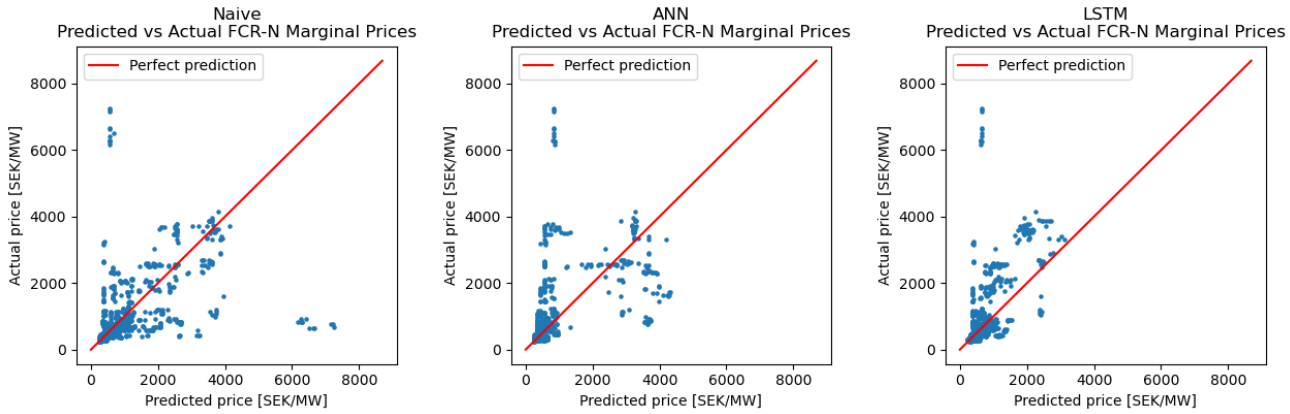


(a) Naive forecast with MAE: 308.2 SEK/MW and MAPE: 37.0 %

(b) ANN forecast with MAE: 375.0 SEK/MW and MAPE: 35.6 %

(c) LSTM forecast with MAE: 292.6 SEK/MW and MAPE: 27.7 %

Figure 21: Marginal FCR-N price forecasting results from the 11th of February to the 14th of April 2024.

### 5.1.3 Average FCR-D Up Price Forecasts

Average FCR-D Up price forecast results are illustrated in Figures 22a-22c. The features used for the ANN forecast are the hour of the day, SE2 spot prices, SE2 hydropower reservoir levels and wind power production. The naive forecast performs best with a MAE of 37 SEK/MW.

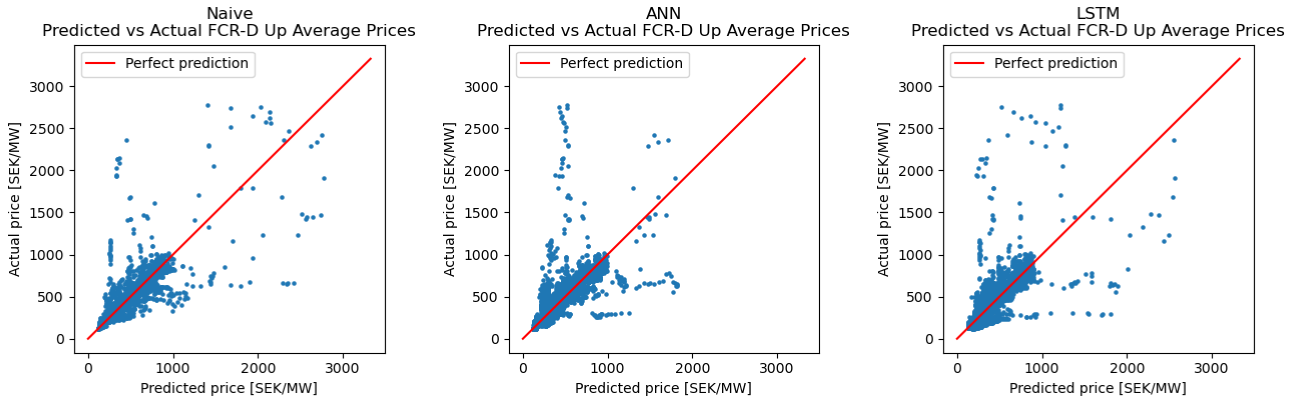


(a) Naive forecast with MAE: 37 SEK/MW and MAPE: 8 %

(b) ANN forecast with MAE: 55.7 SEK/MW and MAPE: 11.6 %

(c) LSTM forecast with MAE: 50.2 SEK/MW and MAPE: 11.1 %

Figure 22: Average FCR-D Up price forecasting results for the year of 2023.

### 5.1.4 Marginal FCR-D Up Price Forecasts

Marginal FCR-D Up price forecast results are illustrated in Figures 23a-23c. The features used for the ANN forecast are the hour of the day and SE2 spot prices. The naive forecast performs best with a MAE of 49 SEK/MW.

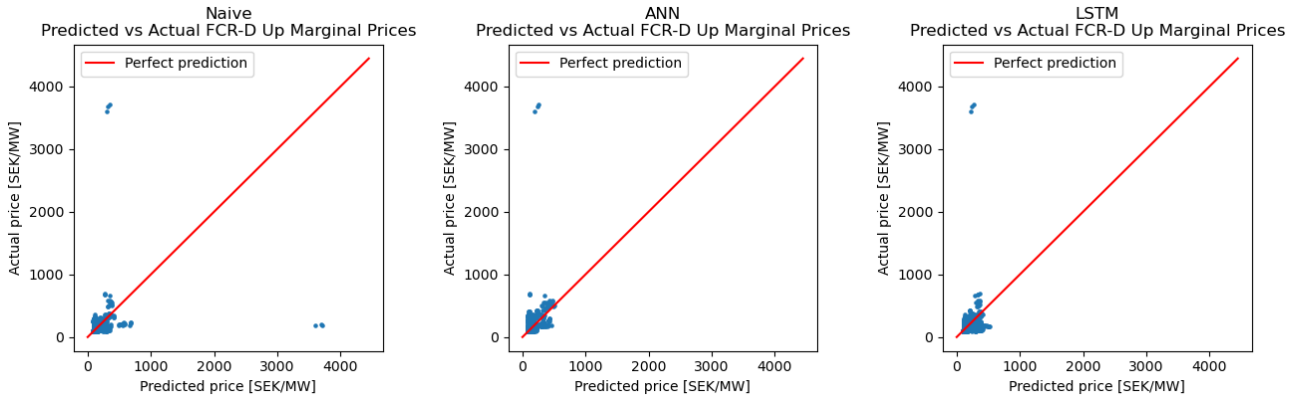


(a) Naive forecast with MAE: 51 SEK/MW and MAPE: 24.2 %

(b) ANN forecast with MAE: 56.1 SEK/MW and MAPE: 27.6 %

(c) LSTM forecast with MAE: 61.5 SEK/MW and MAPE: 39.0 %

Figure 23: Marginal FCR-D Up price forecasting results from the 11th of February to the 14th of April 2024.

### 5.1.5 Average FCR-D Down Price Forecasts

Average FCR-D Down price forecast results are illustrated in Figures 24a-24c. The features used for the ANN forecast are the hour of the day, SE2 spot prices, SE2 hydropower reservoir levels and wind power production. The naive forecast performs best with a MAE of 168 SEK/MW.

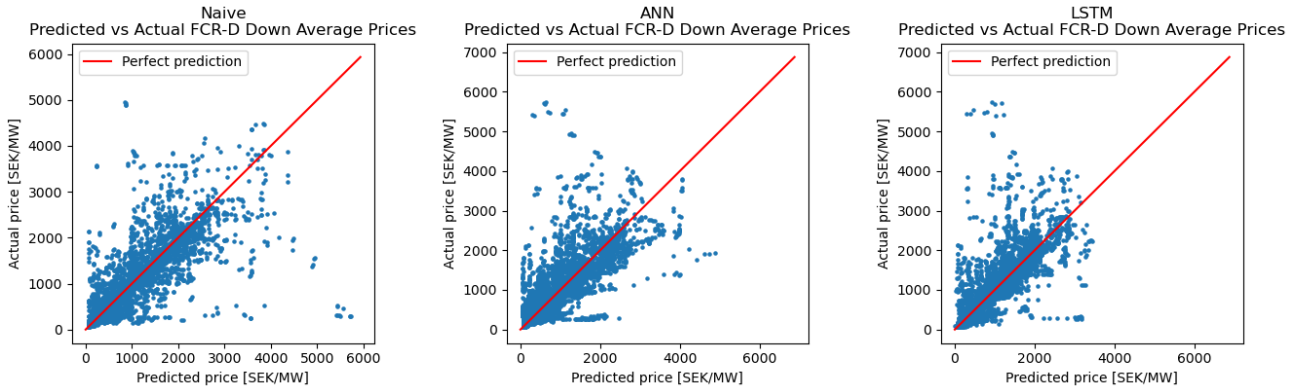


(a) Naive forecast with MAE: 168 SEK/MW and MAPE: 26 %

(b) ANN forecast with MAE: 228.0 SEK/MW and MAPE: 29.3 %

(c) LSTM forecast with MAE: 195.6 SEK/MW and MAPE: 29.5 %

Figure 24: Average FCR-D Down price forecasting results for the year of 2023.

### 5.1.6 Marginal FCR-D Down Price Forecasts

Marginal FCR-D Down price forecast results are illustrated in Figures 25a-25c. The features used for the ANN forecast are SE2 spot prices, SE2 hydropower reservoir level as a percentage of normal levels and the level changes. The LSTM forecast performs best with a MAE of 392.7 SEK/MW.

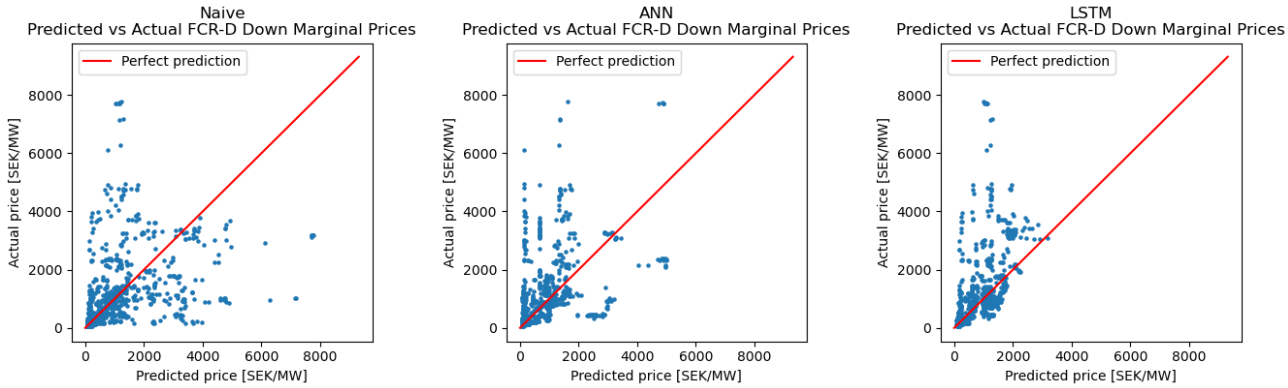


(a) Naive forecast with MAE: 483.0 SEK/MW and MAPE: 74.8 %

(b) ANN forecast with MAE: 473.4 SEK/MW and MAPE: 55.4 %

(c) LSTM forecast with MAE: 358.5 SEK/MW and MAPE: 51.3 %

Figure 25: Marginal FCR-D Down price forecasting results from the 11th of February to the 14th of April 2024.

In Figures 26a-26b the results are summarized by plotting the MAE for each method and price.

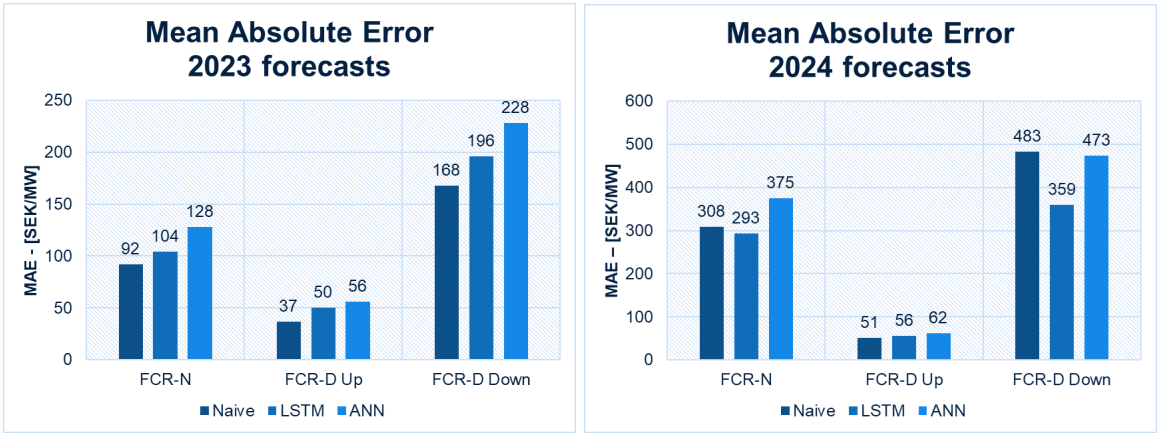


(a) The whole year of 2023.

(b) The 11th of February to the 14th of April 2024.

Figure 26: Mean absolute error results for different forecasted prices for each forecast. Both the average prices during 2023 and marginal prices from the 11th of February to the 14th of April 2024.

## 5.2 Optimization Algorithm

In this section, the optimization algorithm is utilized to conduct analyses aimed at determining the potential profit and identifying the most lucrative markets for participation. Additionally, several sensitivity analyses are performed to assess the impact of various parameters on both the profit margins and the operational dynamics of the BESS.

### 5.2.1 Bid Strategy Comparison

Figures 27-31 present a comparative analysis of various bidding strategies. The figures show the resulting profit and bid allocation among services when the BESS engages in multiple markets. In these analyses, the BESS has a battery capacity of 100 MWh and a power rating of 100 MW. It has a daily initial SOC of 50% and its round-trip efficiency is at 85%. In the figures, the bars show the average hourly bids for each month for each respective forecast. In the strategies when arbitrage is allowed, the revenue from the spot market is at most around 0.3%. Combining FCR and aFRR did not converge to a solution for many dates, hence no results.

In Figure 27, a basic strategy involving constant and uniform FCR-D bids is employed with a constant 50% SOC, resulting in a profit of 875.6 MSEK.

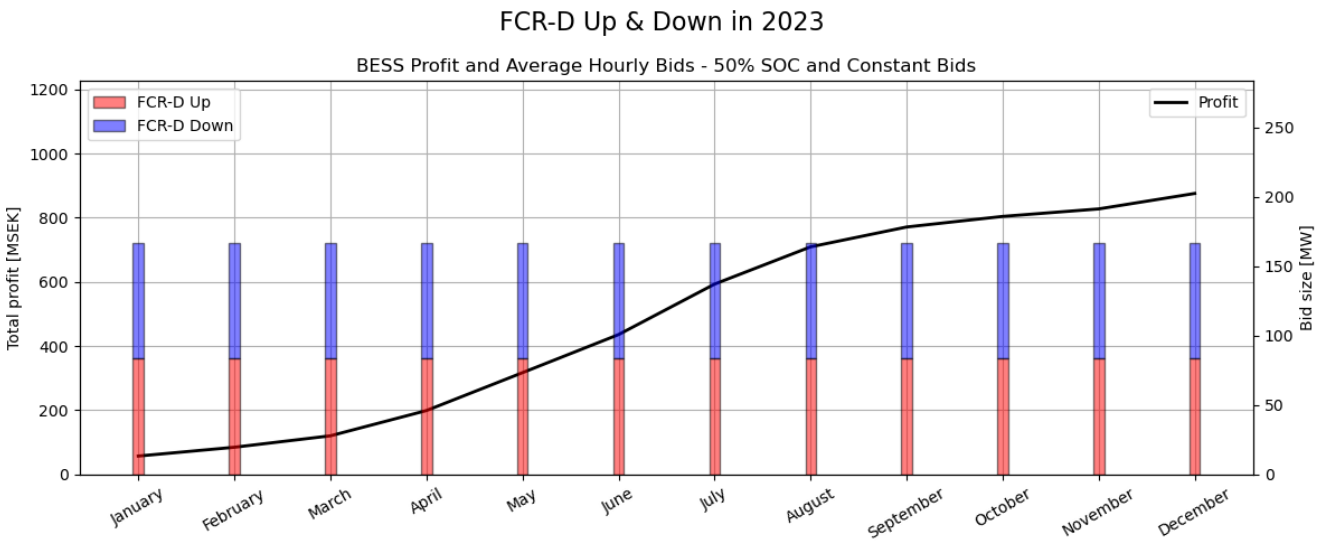


Figure 27: A simple bid strategy of equal FCR-D Up and Down at 50% SOC in 2023.

Utilizing the bid algorithm at constant 50% SOC, optimizing bids with respect to the forecasted regulation service prices, the profit can be increased by 0.318% to 878.4 MSEK when using the naive forecast. Only in July, the profit can be increased by 2.4%. See Figure 28.

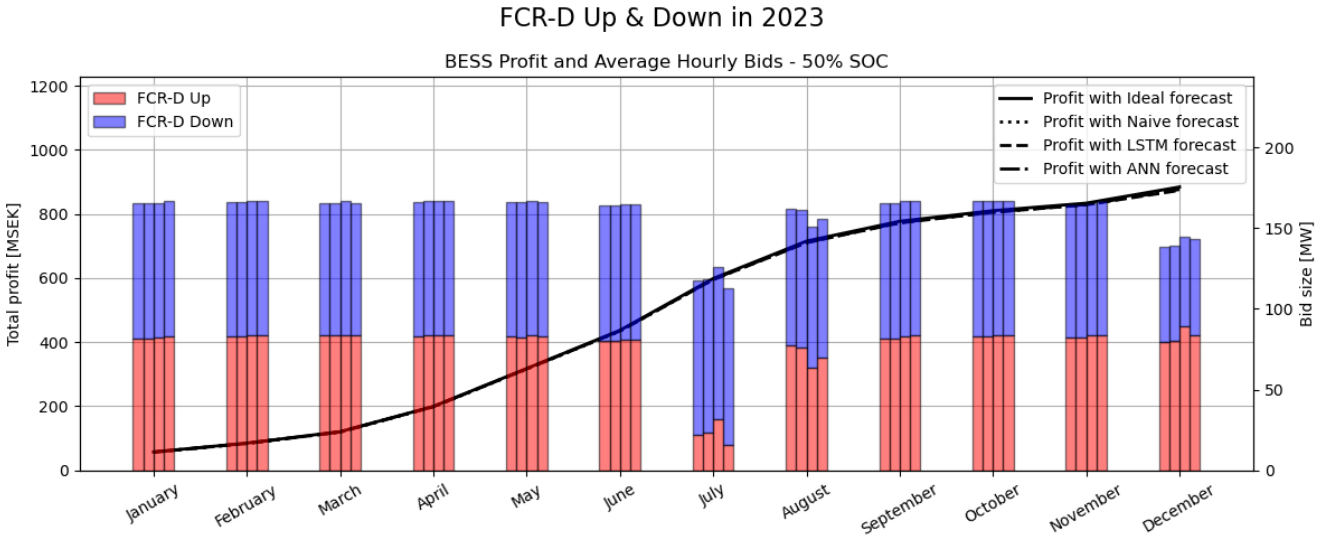


Figure 28: Utilizing the bid algorithm to find optimal FCR-D Up and Down bids at 50% SOC in 2023. The simulated cumulative profit is 884.3, 878.4, 873.6 and 876.5 MSEK for the ideal, naive, LSTM and ANN forecast respectively.

If the BESS is allowed to vary its SOC to the varying prices, adapting to the service prices and performing energy arbitrage, the profit can be increased by 0.337% to 878.5 MSEK when using the naive forecast. See Figure 29.

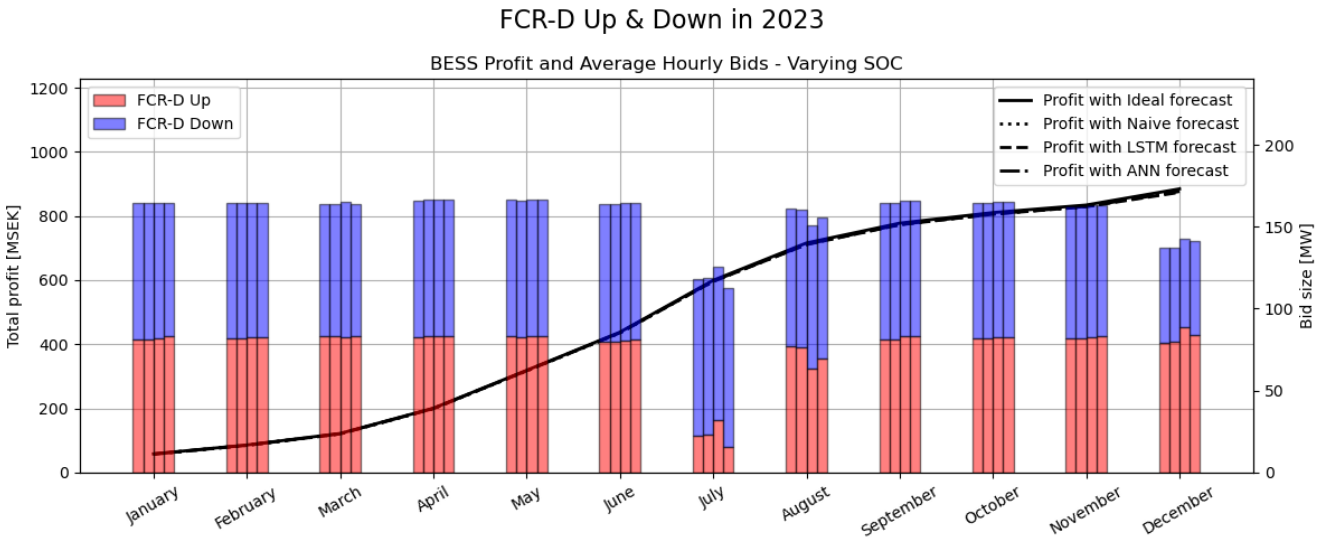


Figure 29: Utilizing the bid algorithm to find optimal FCR-D Up and Down bids while performing arbitrage in 2023. The simulated cumulative profit is 884.6, 878.5, 873.8 and 876.6 MSEK for the ideal, naive, LSTM and ANN forecast respectively.

Allowing the algorithm to include FCR-N while staying at 50% SOC, the profit can be increased by 0.022 % to 875.8 MSEK when using the naive forecast. See Figure 30.

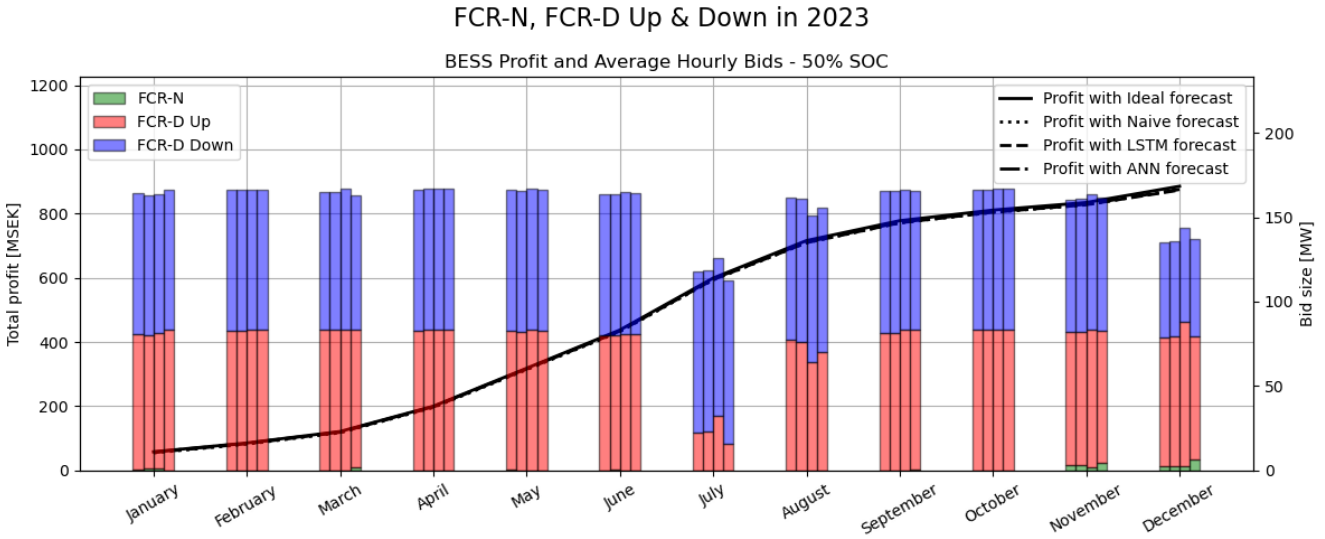


Figure 30: Utilizing the bid algorithm to find optimal FCR-N, FCR-D Up and Down bids at 50% SOC in 2023. The simulated cumulative profit is 885.1, 875.8, 873.1 and 875.0 MSEK for the ideal, naive, LSTM and ANN forecast respectively.

Again, including all FCR services but this time arbitrage is permitted. This decreases profit by 0.172 % to 874.1 MSEK when using the naive forecast. See Figure 31.

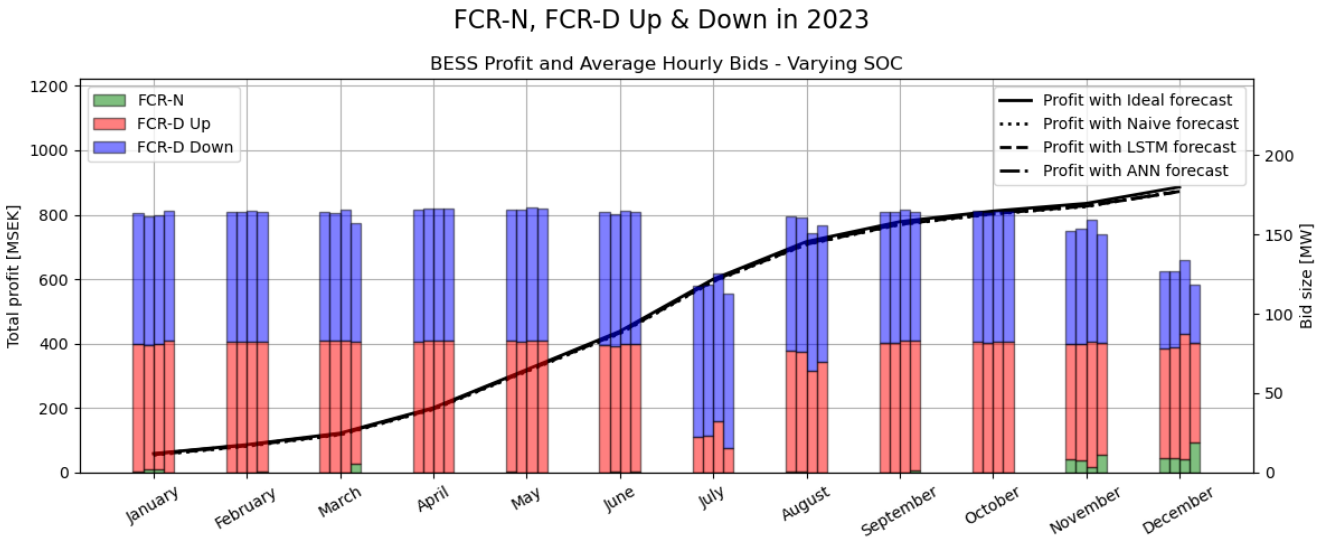


Figure 31: Utilizing the bid algorithm to find optimal FCR-N, FCR-D Up and Down bids while performing arbitrage in 2023. The simulated cumulative profit is 886.4, 874.1, 871.8 and 872.3 MSEK for the ideal, naive, LSTM and ANN forecast respectively.

If the BESS only participates on the aFRR market, the profit becomes 184.0 MSEK for the year of 2023, only 21 % of the basic strategy in Figure 27. See Figure 32.

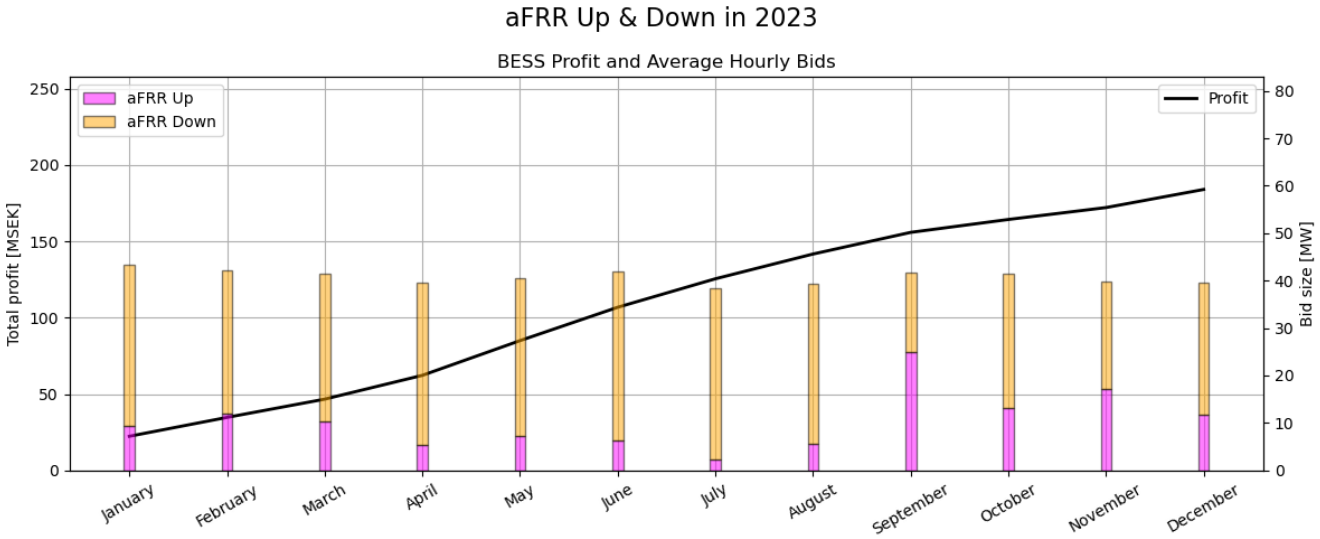


Figure 32: Utilizing the bid algorithm to find optimal aFRR Up and Down bids in 2023. The simulated cumulative profit is 184.0 MSEK.

In Figures 33-34 the results are summarized and the profit is displayed for each strategy and forecast method.

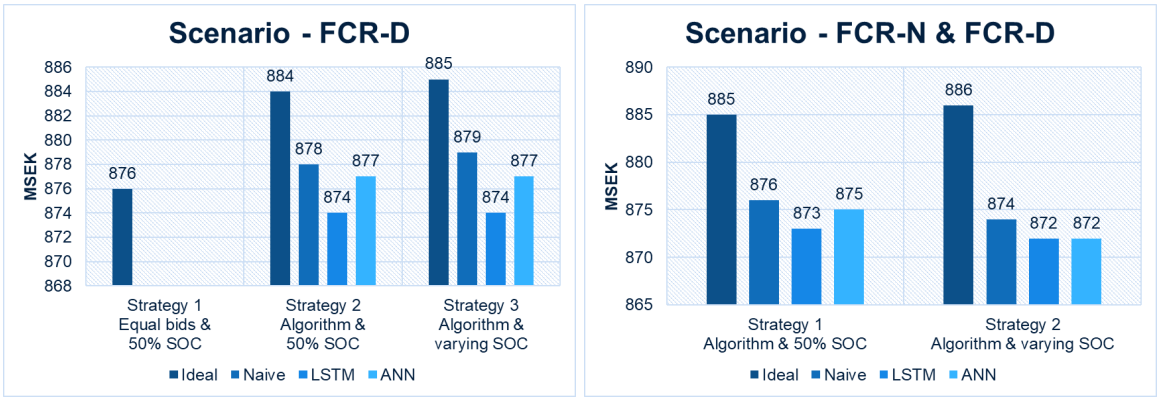


(a) Only FCR-D bids.

(b) FCR-N and FCR-D bids.

Figure 33: Simulated profit comparison between bidding strategies for various forecasting techniques during 2023.

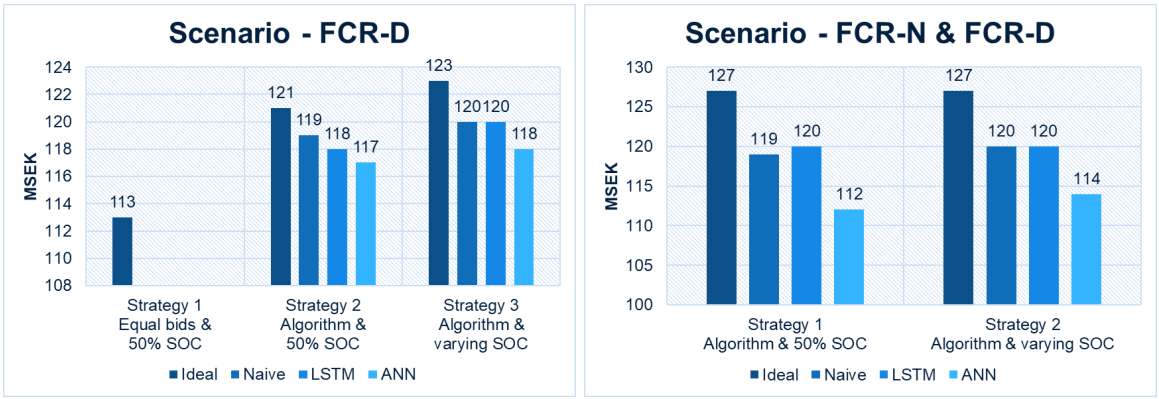


(a) Only FCR-D bids.

(b) FCR-N and FCR-D bids.

Figure 34: Simulated profit comparison between bidding strategies for various forecasting techniques from 11th of February to the 14th of April.

### 5.2.2 Sensitivity Analysis

Multiple analyses for 2023 are undertaken to investigate how adjustments to various parameters impact both profit margins and bid magnitudes. Unless specified otherwise, all other parameters are kept constant throughout the analyses. All prices are assumed to be known. First off, the battery capacity is analysed for FCR and aFRR bids with the results shown in Figures 35 and 36 respectively. Here, a stagnation in profit can be observed at a battery capacity of around 75 MWh for FCR. However, for aFRR, the increased capacity constantly increases profit.

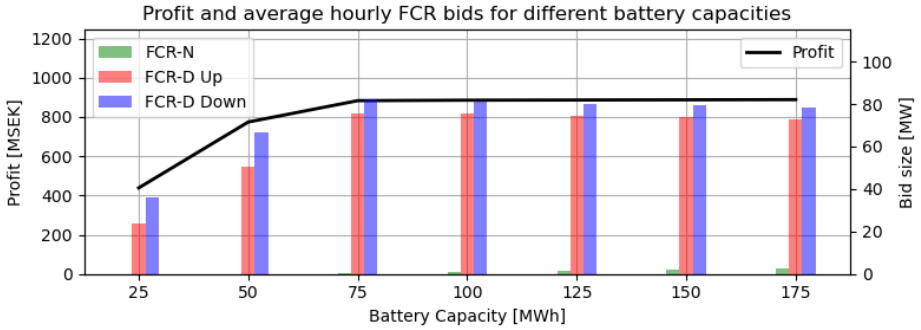


Figure 35: Profit and average hourly FCR bids versus battery capacity during 2023.

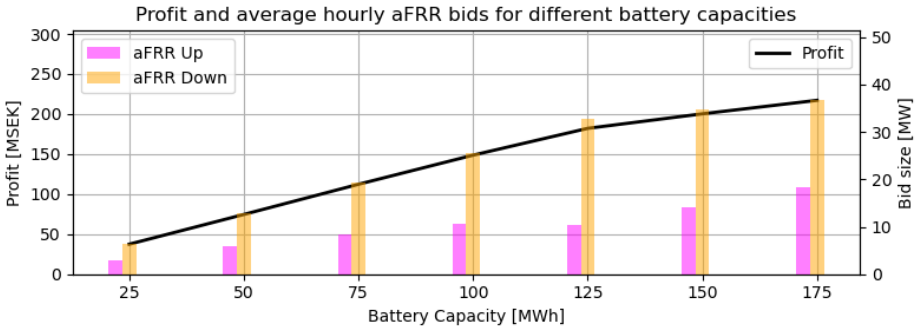


Figure 36: Profit and average hourly aFRR bids versus battery capacity during 2023.

In Figures 37 and 38 the power is varied to assess its influence on the profit and bid sizes. Here, the pattern is reversed compared to Figures 35 and 36.

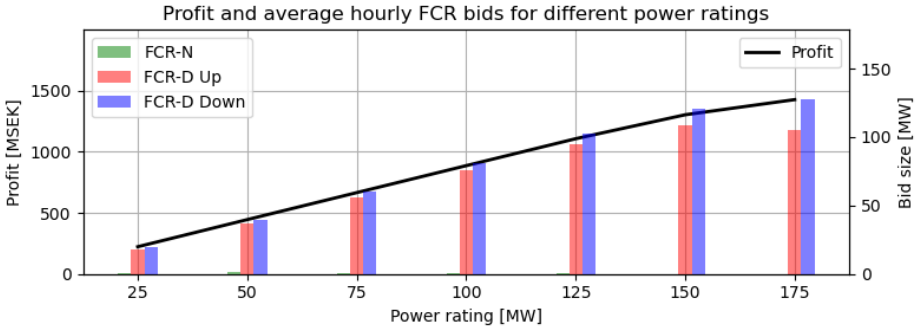


Figure 37: Profit and average hourly FCR bids versus power ratings during 2023.

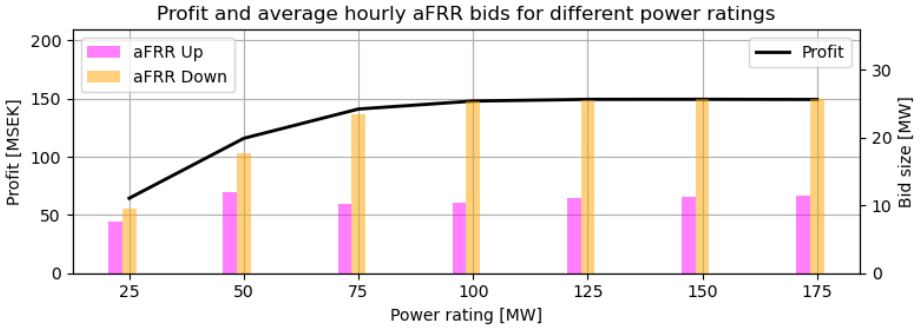


Figure 38: Profit and average hourly aFRR bids versus power ratings during 2023.

Lastly, in Figures 39-41 the service prices are varied. This indicates that a change in FCR-D Down prices has the most significant influence on profit.

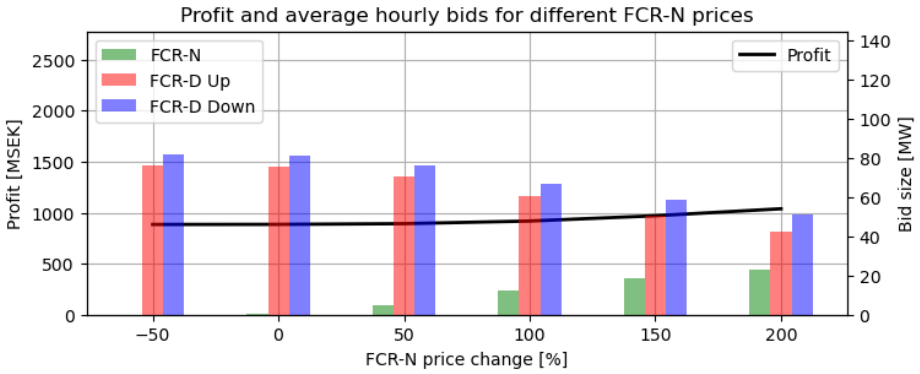


Figure 39: Profit and average hourly FCR bids for different FCR-N prices during 2023.

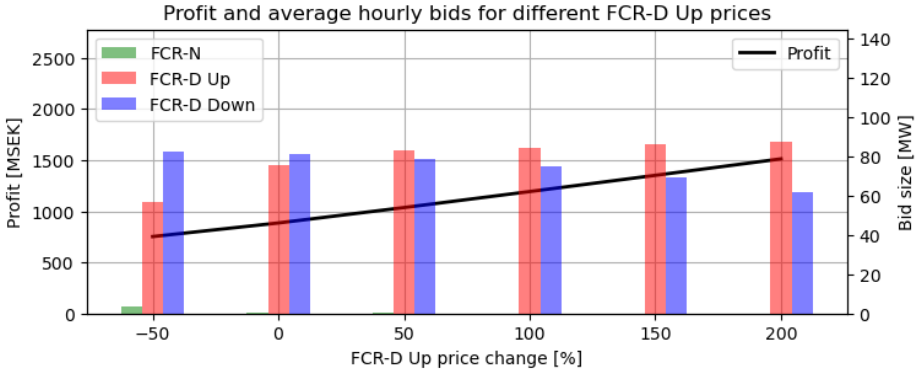


Figure 40: Profit and average hourly FCR bids for different FCR-D Up prices during 2023.

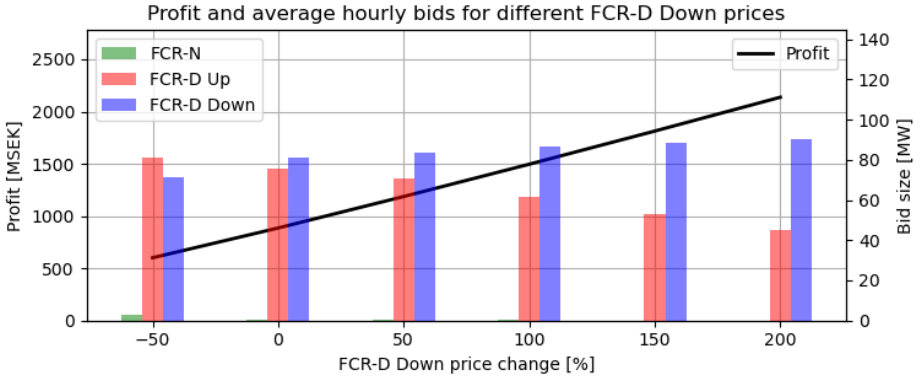


Figure 41: Profit and average hourly FCR bids for different FCR-D Down prices during 2023.

# 6 Discussion and Conclusion

This section provides a comprehensive analysis of the results obtained from the different forecasting models and bidding strategies. The sensitivity analyses are discussed to understand the impact of various factors on profitability. Additionally, directions for future research are proposed to further enhance forecasting accuracy and optimization strategies.

## 6.1 Price Forecasts

Figures 20-25 illustrate the difficulty of accurately forecasting prices. In 2023, the naive forecast performs best overall, but this is not consistently true for all prices in 2024. This is further emphasized in the summary charts in Figure 26. The brief duration of the marginal pricing implementation makes it uncertain whether these conclusions will hold in the long term. For 2024, the naive and LSTM forecasts appear to be the most accurate options.

## 6.2 Bidding Strategies

Figures 33-34 demonstrate that the current bidding strategy is suboptimal and that profits can be increased by employing the bidding algorithm to adjust the ratio of FCR bids. Adapting the SOC to dynamic prices while simultaneously performing energy arbitrage further enhances profitability. In 2023, the similar prices of FCR-D Up and Down for most of the year, except for July, meant the bid algorithm had limited impact, as illustrated in Figures 28-31. Compare with the bid allocation in Figure 27. For the entire year of 2023, the profit could be increased by 0.3% by using the bid algorithm with the naive price forecast, allowing a varying SOC, adapted to the price variations. In July 2023, when the major impact of the bid algorithm was observed, the profit could be increased by 2.4% compared to the profit made from equal bids on FCR-D Up and Down. An even more significant difference is observed from February 1st to April 14th, 2023, where the profit could be increased by 6.2%.

In 2024, higher FCR-N prices, as seen in Figure 18a, make bidding on this service more attractive than in 2023. However, without an improved price forecast, even higher relative prices are necessary to compete with a strategy focused solely on FCR-D bids. Additionally, the larger price difference between FCR-D Up and Down in 2024 advocates for the use of the bid algorithm.

Lastly, it should be mentioned that exclusively participating in the aFRR market is not economically viable, as Figure 32 clearly indicates.

## 6.3 Sensitivity Analysis

The sensitivity analysis in Figure 35 reveals that increasing battery capacity is beneficial only up to approximately 75 MWh, corresponding to a C-rate of 1.33 for a 100 MW BESS. Beyond this point, further increases in battery capacity do not enhance profits because the rated power becomes the limiting factor in bidding, making additional energy reserves redundant. Conversely, below 75 MWh, battery capacity itself is the limiting factor.

In Figure 36, the same is done for aFRR, where the battery capacity consistently being the limiting factor, hence linearly increasing profit as capacity increases. On the other hand, when varying the rated power, as illustrated in Figure 37 and 38, the situation is reversed.

Additionally, Figures 39-41 show that profit is most sensitive to FCR-D Down prices. This sensitivity is due to the comparatively high FCR-D Down prices in 2023, which significantly impact profitability.

## 6.4 Future Research

To enhance the accuracy of forecasts, further experimentation with hyperparameter settings and different LSTM training set sizes is necessary. Additionally, refining the hyperparameter selection process using Bayesian optimization could prove beneficial. Currently, hyperparameters are optimized by minimizing the median of validation losses, but exploring alternatives such as minimizing the mean, trimmed mean, or a specific percentile might yield better results. The choice of optimization metric should align with the desired forecasting goal: whether to prioritize general accuracy at the expense of missing price spikes or to improve spike predictions while accepting higher overall prediction errors.

Access to more powerful computational resources could facilitate the development of more complex models, potentially improving the ability to capture price patterns. However, this must be balanced against the risk of overfitting.

Implementing dimensionality reduction techniques, such as principal component analysis, to preprocess input data for the ANN could also enhance performance.

Advanced forecasting models might benefit from adopting more sophisticated methods, such as multivariate LSTM models using an encoder-decoder architecture. These models could incorporate additional input variables like spot prices, hydropower reservoir data, and temporal features to learn long-term dependencies. Transformer-based models with attention mechanisms represent another promising avenue for improving forecast accuracy.

When devising a bidding strategy, the cost of cycling from FCR-N should be factored in. The bid algorithm could be improved by integrating a battery degradation model, assigning a cost to cycling to avoid excessive bidding on FCR-N. For instance, the battery degradation model provided in the Appendix could be utilized. Additionally, since the optimization problem is solved on a daily basis, the peak shaving strategy could be refined to account for the maximum instantaneous power usage over the entire year.

# References


Battery University. (2023). *Bu-808: How to prolong lithium-based batteries*. Retrieved May 18, 2024, from https://batteryuniversity.com/article/bu-808-how-to-prolong-lithium-based-batteries

Camuñas García-Miguel, P. L., Alonso-Martinez, J., Arnalte, S., Plaza, M., & Peña Asensio, A. (2022). A review on the degradation implementation for the operation of battery energy storage systems. *Batteries*, *8*. https://doi.org/10.3390/batteries8090110

Ellevio. (2024). Elnätspriser företag. Retrieved May 18, 2024, from https://www.ellevio.se/foretag/om-er-el/forsta-er-elnatskostnad/ert-pris/

Energi Informationsservice. (2022). *Effekttariffer och effektavgift*. Retrieved March 2, 2024, from https://ei.se/konsument/el/effekttariffer-effektavgift

Energiföretagen Sverige. (2022). *Energiföretagen förklarar: Hur använder vi el - så varierar priset*. Retrieved February 16, 2024, from https://www.energiforetagen.se/pressrum/nyheter/2022/september/energiforetagen-forklarar-hur-anvander-vi-el--sa-varierar-priset/

Energimarknadsbyrån. (2020, December). *Elområden*. https://www.energimarknadsbyran.se/el/elmarknaden/elomraden/

Energimarknadsinspektionen. (2022). *Ei förklarar: Orsaker bakom svängiga och höga elpriser*. Retrieved February 16, 2024, from https://ei.se/om-oss/nyheter/2022/2022-06-30-ei-forklarar-orsaker-bakom-svangiga-och-hoga-elpriser

Energimyndigheten, S. E. A. (2023). *Uppdaterade långsiktiga scenarier 2023*. Retrieved February 16, 2024, from https://www.energimyndigheten.se/48ea22/globalassets/statistik/prognoser-och-scenarier/langsiktiga-scenarier/uppdaterade-langsiktiga-scenarier-2023.pdf

ENTSO-E. (n.d.). *ENTSO-E*. https://transparency.entsoe.eu/dashboard/show

ENTSO-E. (2022). Energinet and svenska kraftnät proposal for common and harmonised rules and processes for the exchange and procurement of fcr balancing capacity in accordance with article 33(1) of commission regulation (eu) 2017/2195 of 23 november 2017 establishing a guideline on electricity balancing. https://ei.se/download/18.6ac6e41d18093f316201817e/1653997945321/EB-Artikel-33(1)-svenska-kraftn%C3%A4t-metod.pdf

EQ Energy. (2024, May 18). Eq energy: Home. Retrieved May 18, 2024, from https://www.eqenergy.com/

Fingrid. (2022). *Frequency quality analysis 2022* (tech. rep.). Fingrid. https://www.fingrid.fi/globalassets/dokumentit/fi/kantaverkko/suomen-sahkojarjestelma/frequency_quality_analysis_2022_public.pdf

Hashmi, M. U., Labidi, W., Bušić, A., Elayoubi, S.-E., & Chahed, T. (2018). Long-term revenue estimation for battery performing arbitrage and ancillary services. *2018 IEEE International Conference on Communications, Control, and Computing Technologies for Smart Grids (SmartGridComm)*, 1–7. https://doi.org/10.1109/SmartGridComm.2018.8587562

International Energy Agency. (2013). *Nordic energy technology perspectives*. Retrieved February 16, 2024, from https://www.iea.org/reports/nordic-energy-technology-perspectives

Karlsson, F. (2023). *Ankkurvan utmanar det svenska elsystemet*. Retrieved February 16, 2024, from https://polarcapacity.se/ankkurvan-utmanar-det-svenska-elsystemet/

Kochenderfer, M. J., & Wheeler, T. A. (2019). Linear constrained optimization. In *Algorithms for optimization* (pp. 189–210). MIT Press. https://algorithmsbook.com/optimization/files/optimization.pdf

Mimer. (n.d.). Fcr. *Svenska kraftnät*. https://mimer.svk.se/PrimaryRegulation/PrimaryRegulationIndex

Riksbank. (2023). *The swedish electricity market: Today and in the future* (tech. rep.). Riksbank. https://www.riksbank.se/globalassets/media/rapporter/pov/artiklar/engelska/2023/230512/2023_1-the-swedish-electricity-market--today-and-in-the-future.pdf

Skatteverket. (2024). El som återförts till koncessionspliktigt nät efter batterilagring. Retrieved May 18, 2024, from https://www4.skatteverket.se/rattsligvagledning/323435.html#h-El-som-aterforts-till-koncessionspliktigt-nat-efter-batterilagring

Svenska kraftnät. (2021). *Balansering av kraftsystemet*. Retrieved February 16, 2024, from https://www.svk.se/om-kraftsystemet/om-systemansvaret/balansering-av-kraftsystemet/

Svenska kraftnät. (2022, September). *Market handbook nordic afrr capacity market*. https://nordicbalancingmodel.net/wp-content/uploads/2022/08/Nordic-Handbook-aFRR-Capacity-Market.pdf

Svenska kraftnät. (2023a). *Beslut om upphandlingsvolym för frekvenshållningsreserver (fcr) för 2024*. Retrieved March 6, 2024, from https://www.svk.se/press-och-nyheter/nyheter/elmarknad-allmant/2023/beslut-om-upphandlingsvolym-for-frekvenshallningsreserver-fcr-for-2024/

Svenska kraftnät. (2023b). *Delta på fcr- och marknaderna med resurser med begränsad energireserv (ler)*. Retrieved March 2, 2024, from https://www.svk.se/aktorsportalen/bidra-med-reserver/bli-leverantor-av-reserver/bidra-med-fcr-afrr-eller-mfrr/delta-pa-fcr--marknaderna-med-resurser-med-begransad-energireserv--ler/

Svenska kraftnät. (2023c). *Fcr technical requirements*. Svenska kraftnät. Retrieved February 16, 2024, from https://www.svk.se/siteassets/aktorsportalen/bidra-med-reserver/om-olika-reserver/fcr/fcr-technical-requirements-may-23.pdf

Svenska kraftnät. (2023d). *Fifty nordic mms*. Svenska kraftnät. Retrieved February 16, 2024, from https://www.svk.se/aktorsportalen/it-systemsupport/fifty-nordic-mms/

Svenska kraftnät. (2023e). *Frekvenshållningsreserv störning nedreglering (fcr-d ned)*. Svenska kraftnät. Retrieved February 16, 2024, from https://www.svk.se/aktorsportalen/bidra-med-reserver/om-olika-reserver/fcr-d-ned/

Svenska kraftnät. (2023f). *Nordic grid planning data report 2023*. Svenska kraftnät. Retrieved February 16, 2024, from https://www.svk.se/siteassets/om-oss/rapporter/2023/svk_ngpd2023.pdf

Svenska kraftnät. (2023g). *Upphandling av automatisk frekvensåterställningsreserv (afrr) under q2 2023 vecka 14-26*. Svenska kraftnät. Retrieved April 10, 2024, from https://www.svk.se/press-och-nyheter/nyheter/elmarknad-allmant/2023/upphandling-av-automatisk-frekvensaterstallningsreserv-afrr-under-q22023-vecka-14-26/

Svenska kraftnät. (2024a). *Framtida volymbehov*. Svenska kraftnät. Retrieved April 10, 2024, from https://www.svk.se/aktorsportalen/bidra-med-reserver/behov-av-reserver-nu-och-i-framtiden/framtida-volymbehov/

Svenska kraftnät. (2024b). *Frekvensstabilitet*. Svenska kraftnät. Retrieved February 16, 2024, from https://www.svk.se/om-kraftsystemet/om-systemansvaret/kraftsystemstabilitet/frekvensstabilitet/

Svenska kraftnät. (2024c). *När och hur aktiveras afrr?* Retrieved May 17, 2024, from https://www.svk.se/aktorsportalen/bidra-med-reserver/fragor-och-svar-om-reserver/afrr/nar-och-hur-aktiveras-afrr/

Svenska kraftnät. (2024d). *Om olika reserver*. Retrieved May 17, 2024, from https://www.svk.se/aktorsportalen/bidra-med-reserver/om-olika-reserver/

Svenska kraftnät. (2024e). Utbud på marknaderna för reserver. Retrieved May 25, 2024, from https://www.svk.se/aktorsportalen/bidra-med-reserver/behov-av-reserver-nu-och-i-framtiden/utbud-pa-marknaderna-for-reserver/

Svenska kraftnät. (2024f). *Utveckling av elmarknaden*. Svenska kraftnät. Retrieved February 16, 2024, from https://www.svk.se/utveckling-av-kraftsystemet/systemansvar--elmarknad/utveckling-av-elmarknaden/

Svenska kraftnät. (May 23, 2023). *Fcr technical requirements*. Retrieved March 2, 2024, from https://www.svk.se/siteassets/aktorsportalen/bidra-med-reserver/om-olika-reserver/fcr/fcr-technical-requirements-may-23.pdf

Swedish Energy Association. (2017). *Energiåret 2017: Elproduktion*. https://www.energiforetagen.se/4a4eb5/globalassets/energiforetagen/statistik/energiaret/energiaret2017_elproduktion_vers180704.pdf?v=roFaUkzJ0YPsRpp2yIrNswkKIfc&_gl=1*1i8ebav*_up*MQ..*_ga*MTkxNjc2MjEwOS4xNzA5NjU4NzQ0*_ga_RH3QTQ7J0S*MTcwOTY1ODc0My4xLjAuMTcwOTY1ODc0My4wLjAuMA

Swedish Energy Association. (2023). Vattenkraft. Retrieved March 6, 2024, from https://www.energiforetagen.se/energifakta/elsystemet/produktion/vattenkraft/

TN. (2024). *Se upp för högre elpriser*. Retrieved April 9, 2024, from https://www.tn.se/naringsliv/34915/sexdubblad-miljardnota-for-att-balansera-elsystemet-du-far-betala/

Xiong, S. (2019). *Optimization of energy storage system allocation for power grid resilience* [Doctoral dissertation, University of Missouri–Columbia]. Retrieved May 18, 2024, from https://mospace.umsystem.edu/xmlui/bitstream/handle/10355/73777/Xiong-Shihui-Research.pdf

# Appendix

## Degradation

Batteries undergo a decline in both capacity and available power over time due to cycle degradation resulting from usage, and calendar degradation caused by the passage of time. This process can be mitigated by controlling factors such as the Depth Of Discharge (DOD), the rate of charge/discharge, the temperature of the cell, and the SOC (Camuñas García-Miguel et al., 2022). Batteries operating in temperatures well above or below room temperature experience a faster loss of capacity. The State Of Health (SOH) is an important metric and is formulated as

$$SOH = \frac{Cap_{Available}}{Cap_{Nominal}}, \tag{14}$$

where $Cap_{Available}$ is the current available battery capacity and $Cap_{Nominal}$ is the rated battery capacity. The extent of degradation resulting from operation can be determined using the Rainflow Counting Algorithm, stated in Equation (15), which counts and converts partial cycles, or half-cycles $dod_{half}$, into equivalent 100% DOD cycles.

$$T_{cycle} = \sum_{i=1}^{N} \frac{1}{2} (dod_{half})^{k_p} \tag{15}$$

Here, $N$ is the number of half-cycles, and $k_p$ is a degradation constant ranging from 0.8 to 2.1, where a higher $k_p$ value indicates a more resilient battery (Hashmi et al., 2018). The calendar degradation $T_{cal}$ can be calculated as

$$T_{cal} = \frac{T}{L_{cal}}, \tag{16}$$

where $T$ is the time and $L_{cal}$ is the calendar life of the battery. The remaining capacity $Cap_{Available}$ at time $t$ can be calculated from the capacity at time $t-1$ and the loss in calendar and cyclic life $T_{calendar}$ and $T_{cycle}$ respectively.

$$Cap_{available} = Cap_{t-1} - (T_{calendar} + T_{cycle}) Cap_{Nominal} \tag{17}$$

The change in SOH is expressed as

$$\Delta SOH = SOH_t - SOH_{t-1}, \tag{18}$$

and can be used to calculate the degradation cost

$$C^{deg} = \Delta SOH \cdot C^{BESS}, \tag{19}$$

where $C^{BESS}$ is the investment cost. (Camuñas García-Miguel et al., 2022)

When the capacity has been reduced to 80% of its initial capacity, the battery is considered to have reached its end of life. Matching calendar and cycle degradation maximizes the operational life which in turn results in higher economic returns. It is recommended to avoid operation when the economic return is low in order to reduce cycle degradation from surpassing calendar degradation. (Hashmi et al., 2018).

Self discharge is a phenomena where energy is lost due to internal chemical reactions and is increased with age, cycling and temperature. Within 24 hours, a Li-ion battery can under ideal conditions self-discharge 5% from fully charged. Capacity loss and increase in self-discharge is a result of solid electrolyte interphase (SEI), i.e. a layer of lithium oxide and lithium carbonate on the anode which grows with cycling. High SOC can lead to increased SEI growth and electrolyte oxidation on the cathode which aside from capacity loss and increase in self-discharge, increases the internal resistance, resulting in lower discharge capacity and efficiency due to heat dissipation. A temperature of 27° is ideal to maximize battery runtime, higher than that reduces cycle life and lower decreases the discharge capacity. (Xiong, 2019). In [source], a linear extrapolation was used to estimate the degradation for cycling within the SOC ranges [25, 75], [25, 85] and [25, 100]%. Among them, a range of 25% and 75% achieved the best capacity retention, indicating that fully charging the BESS degrades the battery. (Battery University, 2023).